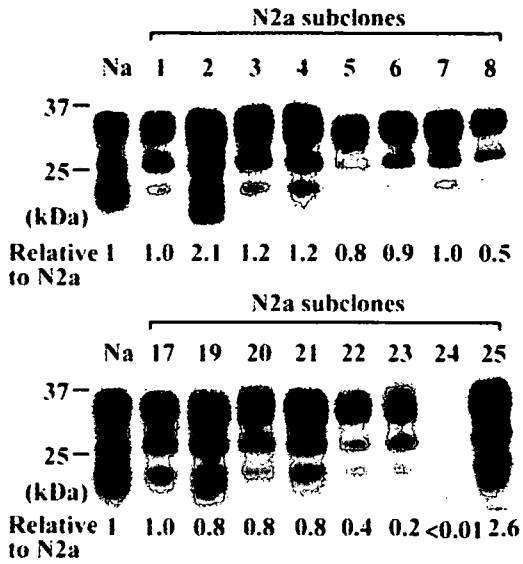

Fig. 2. Expression of PrP^C in N2a subclones. Ten micrograms of cell lysates were loaded on each lane, and PrP^C was detected with mAb 31C6. Na indicates parental N2a cells, and the numbers on the top of the images indicate the number of N2a subclones. Results of representative N2a subclones are indicated. The luminescence intensities were quantified with a LAS-3000 chemiluminescence image analyzer, and the numbers below the images indicate the mean PrP^C expression relative to that in the parental N2a cells (n = 2).

-8, -19, -20, -23, and -24 in Fig. 1) were classified as unsusceptible because they were negative for PrP^{Sc} at all passages examined. Subclones N2a-3 and -5, which showed intense PrP^{Sc} bands at the ninth passage (Fig. 1), were positive for PrP^{Sc} for more than 30 serial passages (data not shown). Thus, we used N2a-3 and -5 as representative prion-susceptible N2a subclones in the following experiments.

Expression of PrP^C and PrP Gene

Because PrP^C is essential for the propagation of prion and formation of PrP^{Sc} (5–7), we first investigated PrP^C expression in N2a subclones by WB (Fig. 2). As expected, prion-susceptible subclones expressed 0.4- to 2.6-fold as much PrP^C as the parental N2a cells (Fig. 2). Among the prion-susceptible subclones, N2a-22 showed the lowest PrP^C expression; it expressed only 0.4 ± 0.1-fold as much PrP^C as the parental N2a cells. In contrast, PrP^C expression varied among the prion-unsusceptible subclones. For instance, subclones N2a-1, -4, -8, -19, and -20 expressed similar level of PrP^C as the parental N2a cells and susceptible subclones, whereas N2a-23 and -24 had lower PrP^C expression than the parental cells, and actually, subclone N2a-24 expressed only one one-hundredth as much PrP^C as the parental N2a cells.

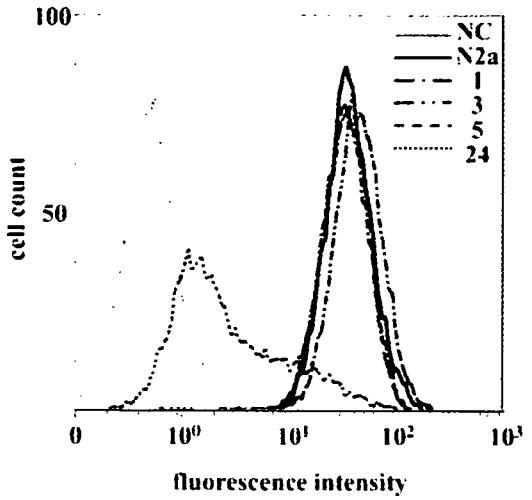

Fig. 3. Cell surface expression of PrP^C in N2a subclones. PrP^C on the cell surface of N2a and subclones N2a-1, -3, -5, and -24 was detected by flow cytometry. NC indicates the fluorescence intensity of N2a cells stained with negative control mAb P1-284 as a primary antibody. The PrP^C expression levels relative to that in parental N2a cells were calculated from mean fluorescence intensities and are shown in Table 1.

Table 1. Levels of PrP^C and PrP mRNA expression in N2a subclones

N2a subclone	Relative to parental N2a cells		
	Total $PrP^{C\,a)}$	PrPC on cell surface[a)]	PrP mRNA[a)]
N2a-1	1.0 ± 0.7	1.1 ± 0.06	1.4 ± 0.4
N2a-3	1.2 ± 0.5	1.3 ± 0.07	1.8 ± 0.7
N2a-5	0.8 ± 0.2	1.0 ± 0.06	1.5 ± 0.4
N2a-24	0.01 ± 0.004	0.07 ± 0.006	0.1 ± 0.04

[a)] Means ± S.D. (n=3) relative to parental N2a cells.

Flow cytometric analysis showed that susceptible subclones N2a-3 and -5, and the unsusceptible subclone N2a-1 expressed PrP^C on their cell surfaces, whereas, consistent with the WB analysis, the level of PrP^C on the cell surface of the N2a-24 subclone was less than one-tenth of that in parental N2a cells (Fig. 3, Table 1). Furthermore, quantitative RT-PCR analysis also showed that the expression of the PrP gene in N2a-1, -3, and -5 was 1.4-, 1.8-, and 1.5-fold higher than in the parental N2a cells, respectively, whereas N2a-24 expressed only one-tenth as much PrP mRNA as the parental N2a cells (Table 1). Thus, the low level of PrP^C expression in N2a-24 is probably due to inefficient transcription of the PrP gene. These results indicated that there are two types of prion-unsusceptible N2a subclones: one (e.g., N2a-1) that expresses a level of PrP^C similar to prion-susceptible N2a cells, and another (e.g., N2a-24) that

expresses lower levels of PrP^C than susceptible cells.

Cellular Cholesterol Content of N2a Subclones

The cellular cholesterol is reported to be important for the accumulation of PrP^{Sc} in prion-infected N2a cells (2, 38). We therefore measured the cellular cholesterol content in representative N2a subclones; however, there was no significant difference in the cellular cholesterol contents between the parental N2a cells (8.3 ± 0.9 μg/mg protein), prion-unsusceptible subclones N2a-1 and -24 (8.6 ± 0.7 and 9.3 ± 0.9 μg/mg protein, respectively) and susceptible subclones N2a-3 and -5 (9.2 ± 0.4 and 7.9 ± 0.9 μg/mg protein, respectively).

Binding of PrP^{Sc} to N2a Subclones

Binding of PrP^{Sc} to the cells is considered to be the initial step in the prion infection after cells are inoculated with prion-infected brain homogenates. Thus, we examined the binding of PrP^{Sc} to N2a subclones to investigate whether the binding step is involved in determining the prion-susceptibility and whether the expression of PrP^C affects PrP^{Sc} binding. Figure 4a shows the representative results for the binding of PrP^{Sc} to N2a subclones at 37 C. PrP^{Sc} bound equally to prion-susceptible (N2a-3 and -5) and unsusceptible N2a subclones (N2a-1 and -24). In addition, there was no significant difference in the amount of bound PrP^{Sc} among N2a subclones and N2aII/9-4 that of stably overexpressed mouse PrP^C (Fig. 5a). In addition, we observed a dose-dependent increase in PrP^{Sc} binding both on ice and at 37 C, regardless of the prion susceptibility or level of PrP^C in the cells (Fig. 4b). The increase of bound PrP^{Sc} at 37 C suggests that a part of bound PrP^{Sc} may be internalized during the incubation. These results revealed that prion susceptibility of these subclones is not determined by the binding and/or uptake of PrP^{Sc} and that PrP^C is not directly involved in the binding and/or uptake of PrP^{Sc}.

Effect of Exogenously Introduced PrP^C on Prion Susceptibility

We speculated that the low level of PrP^C expression in N2a-24 may explain its inability to support prion replication. To examine this possibility, we transfected N2a-1 and -24 cells with the mouse PrP gene expression vector pRc/EF-MoPrP and selected stable transformants in the presence of G418. We also used the PrP^C-overexpressing N2a subclone N2aII/9-4, which is a stable transformant by pRc/EF-MoPrP, as a control for G418-resistant prion-susceptible cells. Quantitative analysis of

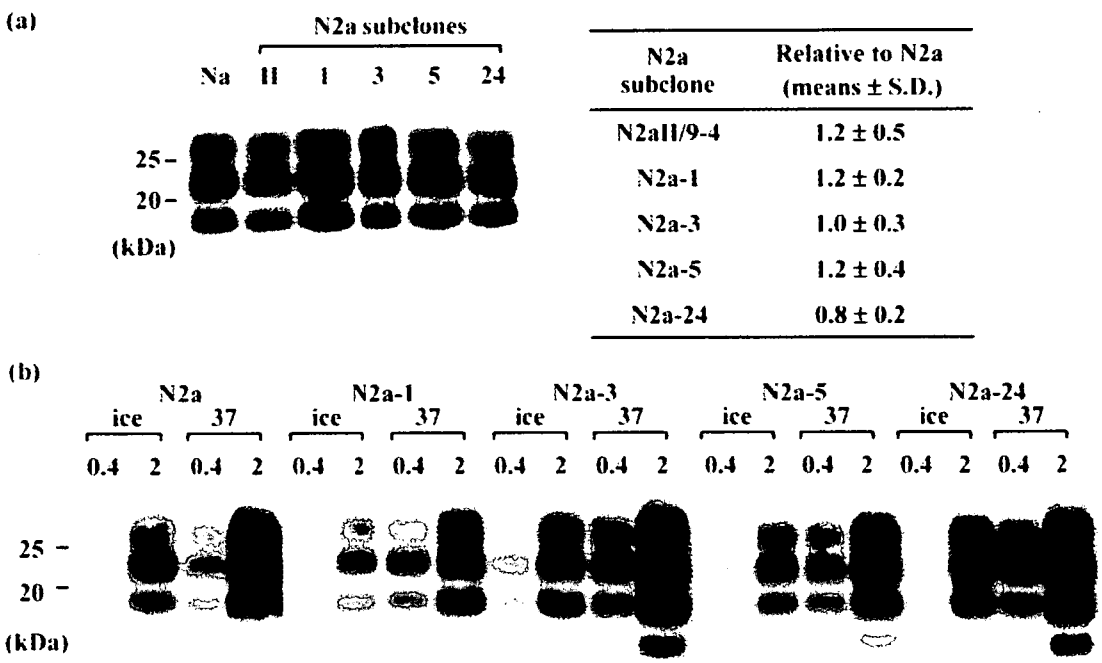

N2a subclone	Relative to N2a (means ± S.D.)
N2aII/9-4	1.2 ± 0.5
N2a-1	1.2 ± 0.2
N2a-3	1.0 ± 0.3
N2a-5	1.2 ± 0.4
N2a-24	0.8 ± 0.2

Fig. 4. Binding of PrP^{Sc} to N2a subclones. (a) Representative results for the binding of PrP^{Sc} to N2a cells. The cells were inoculated with 2% brain homogenate from mice infected with Chandler strain and then incubated at 37 C for 3 hr. Bound PrP^{Sc} was detected as described in "Materials and Methods." The binding of PrP^{Sc} relative to that in parental N2a cells is shown in the table on the right. Values in the table are the means ± S.D. from three independent experiments. Na, parental N2a cells; II, N2aII/9-4; 1, 3, 5, and 24, N2a subclone-1, -3, -5, and -24, respectively. (b) Dose- and temperature-dependent binding of PrP^{Sc}. The cells were inoculated with 0.4 and 2% brain homogenate from mice infected with Chandler strain and incubated at 37 C or on ice for 3 hr.

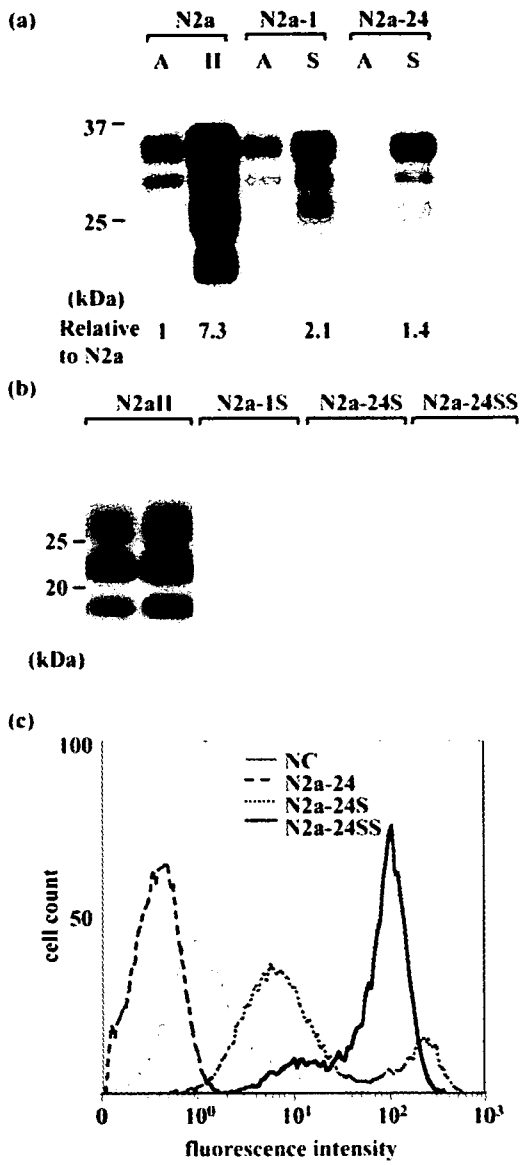

Fig. 5. (a) Expression of PrP^C in N2a, N2a-1, and N2a-24 cells. N2a-1 and N2a-24 subclones were transfected with pRc/EF-MoPrP, and G418-resistant cells were selected. A indicates authentic cells, and S indicates G418-resistant cells. The G418-resistant N2a subclone II/9-4 was used as a control for G418-resistant prion-susceptible cells. Ten micrograms of the cell lysates were loaded on each lane, and PrP^C was detected with mAb 31C6. The luminescence intensities were quantified, and the numbers below the image indicate the amount of PrP^C relative to that in N2a cells. (b) Effect of PrP^C expression on prion susceptibility of subclones N2a-1 and N2a-24. N2aII/9-4, N2a-1S, and N2a-24S cells were inoculated with 2% brain homogenate from mice infected with Chandler strain. PrP^{Sc} was detected after the sixth consecutive passage. The results of duplicate samples are shown. (c) Cell surface expression of PrP^C in N2a-24 cells. PrP^C on the cell surface of N2a-24, 24S, and 24SS (selected by cell sorter) was detected by flow cytometry. NC indicates the fluorescence intensity of N2a-24S cells stained with negative control mAb P1-284 as a primary antibody.

WB revealed that the G418-resistant N2a-1 (N2a-1S) and N2a-24 (N2a-24S) cells expressed 2.1- and 1.4-fold more PrP^C than the parental N2a cells (Fig. 5a). In addition, the G418-resistant N2a subclone N2aII/9-4 expressed 7.3-fold more PrP^C than parental N2a cells. Flow cytometric analysis revealed that 39% of N2a-1S (data not shown) and 32% of N2a-24S cells expressed higher surface level of PrP^C than the corresponding authentic subclones (Fig. 5c). These cells were inoculated with brain homogenate from prion-infected mice and then examined for PrP^{Sc} after six serial passages. PrP^{Sc} was detected in neither N2a-1S nor N2a-24S cells but was detected in N2aII/9-4 cells, suggesting that stable expression of PrP^C did not confer the prion susceptibility to N2a-1 and N2a-24 cells (Fig. 5b). The fact that 32% of G418-resistant N2a-24S cells expressed elevated levels of PrP^C might cause the inefficient prion replication in N2a-24S cells. To exclude this possibility, we collected PrP^C-overexpressing cells from G418-resistant N2a-24S cells by cell sorting. In this cell population (N2a-24SS), 79% of cells expressed elevated cell surface levels of PrP^C (Fig. 5c); however, PrP^{Sc} was not detected in these cells when they were inoculated with prion-infected brain homogenates (data not shown).

Discussion

N2a cells have been reported to be composed of cells with different susceptibilities to prion infection (4, 9). One of the determinants of prion susceptibility is the expression of PrP^C (3–5), but the quantitative relationship between PrP^C expression and prion susceptibility is not well understood. We found considerable variation in the expression of PrP^C in the N2a subclones established in this study. In particular, subclone N2a-24 expressed less than one one-hundredth as much PrP^C as the parental N2a cells. Among the prion-susceptible N2a subclones, N2a-22 showed the lowest expression of PrP^C but still expressed 0.4-fold as much PrP^C as the parental N2a cells, suggesting that a substantial amount of PrP^C is required to support prion propagation in N2a subclones. On the other hand, as represented by subclone N2a-1, some prion-unsusceptible subclones expressed similar levels of PrP^C as the parental N2a cells and other prion-susceptible subclones. These results are consistent with the idea that the expression of PrP^C is a critical factor but they also indicate that other factors and/or cellular microenvironments also determine the susceptibility of N2a cells to prion (4).

Exposing cells to prion-infected materials such as brain homogenates usually starts infection, and many cell lines can bind and internalize exogenous PrP^{Sc} (24, 25, 39). Recently, Hijazi et al. showed that the similar

levels of PrP^{Sc} bind to wild-type Chinese hamster ovary (CHO) cells, which do not express detectable levels of PrP^C, and CHO cells overexpressing PrP^C (13). Magalhaes et al. also showed that uptake of exogenous PrP^{Sc} does not require the presence of endogenous PrP^C (25). In agreement with these observations, our results indicated that the binding of exogenous PrP^{Sc} to the N2a cells was neither related to the prion susceptibility nor the level of PrP^C expression. This also indicated that the binding of PrP^{Sc} observed in this study did not account for the specific binding to PrP^C but binding of PrP^{Sc} to cell surface, although molecules and microenvironments involved in the binding are unclear. Cellular heparan sulfate (HS) has been reported to be involved in the uptake of exogenous PrP^{Sc} following productive prion propagation in cells (14). In addition, the complex of LRP/LR and HS proteoglycan has been suggested to act as a receptor for PrP^{Sc} (12, 15). We did not address the role of LRP/LR and HS proteoglycan in the binding of PrP^{Sc} to N2a subclones; however, when the binding assay was carried out at 37 C, PrP^{Sc} binding to the N2a subclones was increased regardless of the PrP expression level or prion susceptibility, suggesting that the uptake of PrP^{Sc} may not be a major determinant of prion susceptibility in the N2a subclones. A recent report showed that the trafficking of exogenous PrP^{Sc} in mouse septum neuron-derived SN56 cells differed according to the ability of prion to propagation in the cells (25). This suggested that prion susceptibility may be determined by events occurring after the uptake of PrP^{Sc}. Therefore it would be of interest to analyze the fate of PrP^{Sc} after its binding to prion-susceptible and -unsusceptible N2a subclones.

In this study, we obtained a subclone, N2a-24, in which the expression of PrP^C was much lower than in the parental N2a cells and other subclones. We confirmed that the low PrP^C expression was due to inefficient expression of PrP mRNA. To address whether the low level of PrP gene expression is caused by genomic mutations in the regions involved in transcription of the PrP gene, we used long PCR to amplify the 5'- and 3'-flanking regions of exon 1 (nucleotides 6055–12058 in accession number U29186), which contain regions influencing PrP gene expression (17, 33) and carried out a direct sequencing of the amplified products. We did not find any nucleotide differences in this region between authentic N2a cells and subclones N2a-5 and N2a-24. We further analyzed the nucleotide sequences of exon 3 and its flanking regions (nucleotides 27096–30189 in accession number U29186), but again, the sequences were identical in authentic N2a cells and subclones N2a-5 and N2a-24 (data not shown). Thus, the low level of PrP gene expression in N2a-24 was not due to a mutation in the PrP gene but rather was probably due to a deficiency in the cellular machinery used for transcription of the PrP gene. In hepatic stellate cells, which express trace amounts of PrP^C, the expression of PrP^C increased in response to CCl_4-induced hepatic damage (16). In addition, PrP^C expression is increased in peripheral nerves during axon regeneration (28). These studies raised the possibility that the regulation of PrP^C expression plays a role in neural and hepatic regeneration. In addition, PrP gene expression is developmentally regulated (26), but the molecular mechanism controlling PrP gene expression remains unclear. Thus, the low expression of the PrP gene in subclone N2a-24 despite a lack of mutations in the genomic region of the PrP gene, suggests that this subclone will be useful for analyzing the mechanism of PrP gene expression.

Host factors other than PrP^C may be involved in the PrP^{Sc} formation, i.e., prion replication, but little is known so far. A comparison of prion-susceptible and -resistant tissues could help to identify such host factors; however, large differences exist in gene expression profiles between tissues and thus comparison between tissues would complicate the identification of factors influencing prion susceptibility. A fine comparison would be possible, however, if the compared samples have similar biological properties. Hence, the N2a subclones established in this study should be useful for identifying host factors and cellular microenvironments influencing prion replication. Comprehensive comparison of these cells by transcriptomic and proteomic analyses will be useful in this regard and should help to elucidate the molecular mechanism of prion replication.

This work was supported by a grant from The 21st Century COE Program (A-1) and a Grant-in-Aid for Science Research (A) (grant 15208029) from the Ministry of Education, Culture, Sports, Science and Technology, Japan. This work was also supported by a grant from the Ministry of Health, Labour and Welfare, Japan.

References

1) Applied Biosystems: User Bulletin #2 ABI Prism 7700 Sequence Detection System: December 11, 1997.
2) Bate, C., Salmona, M., Diomede, L., and Williams, A. 2004. Squalestatin cures prion-infected neurons and protects against prion neurotoxicity. J. Biol. Chem. **279**: 14983–14990.
3) Borchelt, D.R., Scott, M., Taraboulos, A., Stahl, N., and Prusiner, S.B. 1990. Scrapie and cellular prion proteins differ in their kinetics of synthesis and topology in cultured cells. J. Cell Biol. **110**: 743–752.
4) Bosque, P.J., and Prusiner, S.B. 2000. Cultured cell sublines highly susceptible to prion infection. J. Virol. **74**:

4377–4386.
5) Brandner, S., Raeber, A., Sailer, A., Blattler, T., Fischer, M., Weissmann, C., and Aguzzi, A. 1996. Normal host prion protein (PrPC) is required for scrapie spread within the central nervous system. Proc. Natl. Acad. Sci. U.S.A. **93**: 13148–13151.
6) Büeler, H., Aguzzi, A., Sailer, A., Greiner, R.A., Autenried, P., Aguet, M., and Weissmann, C. 1993. Mice devoid of PrP are resistant to scrapie. Cell **73**: 1339–1347.
7) Büeler, H., Fisher, M., Lang, Y., Bluethmann, H., Lipp, H.P., DeArmond, S.J., Prusiner, S.B., Aguet, M., and Weissmann, C. 1992. Normal development and behavior of mice lacking the neuronal cell-surface PrP protein. Nature **356**: 577–582.
8) Caughey, B., and Raymond, G.J. 1991. The scrapie-associated form of PrP is made from a cell surface precursor that is both protease- and phospholipase-sensitive. J. Biol. Chem. **266**: 18217–18223.
9) Enari, M., Flechsig, E., and Weissmann, C. 2001. Scrapie prion protein accumulation by scrapie-infected neuroblastoma cells abrogated by exposure to a prion protein antibody. Proc. Natl. Acad. Sci. U.S.A. **98**: 9295–9299.
10) Ertmer, A., Gilch, S., Yun, S.W., Flechsig, E., Klebl, B., Stein-Gerlach, M., Klein, M.A., and Schatzl, H.M. 2004. The tyrosine kinase inhibitor STI571 induces cellular clearance of PrP(Sc) in prion-infected cells. J. Biol. Chem. **279**: 41918–41927.
11) Fischer, M.B., Roeckl, C., Parizek, P., Schwarz, H.P., and Aguzzi, A. 2000. Binding of disease-associated prion protein to plasminogen. Nature **408**: 479–483.
12) Gauczynski, S., Nikles, D., El-Gogo, S., Papy-Garcia, D., Rey, C., Alban, S., Barritault, D., Lasmezas, C.I., and Weiss, S. 2006. The 37-kDa/67-kDa laminin receptor acts as a receptor for infectious prions and is inhibited by polysulfated glycanes. J. Infect. Dis. **194**: 702–709.
13) Hijazi, N., Kariv-Inbal, Z., Gasset, M., and Gabizon, R. 2005. PrPSc incorporation to cells requires endogenous glycosaminoglycan expression. J. Biol. Chem. **280**: 17057–17061.
14) Horonchik, L., Tzaban, S., Ben-Zaken, O., Yedidia, Y., Rouvinski, A., Papy-Garcia, D., Barritault, D., Vlodavsky, I., and Taraboulos, A. 2005. Heparan sulfate is a cellular receptor for purified infectious prions. J. Biol. Chem. **280**: 17062–17067.
15) Hundt, C., Peyrin, J.M., Haik, S., Gauczynski, S., Leucht, C., Rieger, R., Riley, M.L., Deslys, J.P., Dormont, D., Lasmezas, C.I., and Weiss, S. 2001. Identification of interaction domains of the prion protein with its 37-kDa/67-kDa laminin receptor. EMBO J. **20**: 5876–5886.
16) Ikeda, K., Kawada, N., Wang, Y.Q., Kadoya, H., Nakatani, K., Sato, M., and Kaneda, K. 1998. Expression of cellular prion protein in activated hepatic stellate cells. Am. J. Pathol. **153**: 1695–1700.
17) Inoue, S., Tanaka, M., Horiuchi, M., Ishiguro, N., and Shinagawa, M. 1997. Characterization of the bovine prion protein gene: the expression requires interaction between the promoter and intron. J. Vet. Med. Sci. **59**: 175–183.
18) Kaneko, K., Zulianello, L., Scott, M., Cooper, C.M., Wallace, A.C., James, T.L., Cohen, F.E., and Prusiner, S.B. 1997. Evidence for protein X binding to a discontinuous epitope on the cellular prion protein during scrapie prion propagation. Proc. Natl. Acad. Sci. U.S.A. **94**: 10069–10074.
19) Kim, C.L., Karino, A., Ishiguro, N., Shinagawa, M., Sato, M., and Horiuchi, M. 2004. Cell-surface retention of PrP(C) by anti-PrP antibody prevents protenase-resistant PrP formation. J. Gen. Virol. **85**: 3473–3482.
20) Kim, C.L., Umetani, A., Matui, T., Ishiguro, N., Shinagawa, M., and Horiuchi, M. 2004. Antigenic characterization of an abnormal isoform of prion protein using a new diverse panel of monoclonal antibodies. Virology **320**: 40–51.
21) Kurschner, C., and Morgan, J.I. 1995. The cellular prion protein (PrP) selectively binds to Bcl-2 in the yeast two-hybrid system. Brain Res. Mol. Brain Res. **30**: 165–168.
22) Leucht, C., Simoneau, S., Rey, C., Vana, K., Rieger, R., Lasmezas, C.I., and Weiss, S. 2003. The 37 kDa/67 kDa laminin receptor is required for PrP(Sc) propagation in scrapie-infected neuronal cells. EMBO Rep. **4**: 290–295.
23) Luhr, K.M., Nordstrom, E.K., Low, P., and Kristensson, K. 2004. Cathepsin B and L are involved in degradation of prions in GT1-1 neuronal cells. NeuroReport **15**: 1663–1667.
24) Luhr, K.M., Wallin, R.P., Ljunggren, H.G., Low, P., Taraboulos, A., and Kristensson, K. 2002. Processing and degradation of exogenous prion protein by CD11c(+) myeloid dendritic cells *in vitro*. J. Virol. **76**: 12259–12264.
25) Magalhaes, A.C., Baron, G.S., Lee, K.S., Steele-Mortimer, O., Dorward, D., Prado, M.A., and Caughey, B. 2005. Uptake and neuritic transport of scrapie prion protein coincident with infection of neuronal cells. J. Neurosci. **25**: 5207–5216.
26) Manson, J., West, J.D., Thomson, V., McBride, P., Kaufman, M.H., and Hope, J. 1992. The prion protein gene: a role in mouse embryogenesis? Development **115**: 117–122.
27) Mizushima, S., and Nagata, S. 1990. pEF-BOS, a powerful mammalian expression vector. Nucleic Acids Res. **18**: 5322.
28) Moya, K.L., Hassig, R., Breen, K.C., Volland, H., and Di Giamberardino, L. 2005. Axonal transport of the cellular prion protein is increased during axon regeneration. J. Neurochem. **92**: 1044–1053.
29) Naslavsky, N., Stein, R., Yanai, A., Friedlander, G., and Taraboulos, A. 1997. Characterization of detergent-insoluble complexes containing the cellular prion protein and its scrapie isoform. J. Biol. Chem. **272**: 6324–6331.
30) Nordstrom, E.K., Luhr, K.M., Ibanez, C., and Kristensson, K. 2005. Inhibitors of the mitogen-activated protein kinase kinase 1/2 signaling pathway clear prion-infected cells from PrPSc. J. Neurosci. **25**: 8451–8456.
31) Prusiner, S.B. 1991. Molecular biology of prion diseases. Science **252**: 1515–1522.
32) Rieger, R., Edenhofer, F., Lasmezas, C.I., and Weiss, S. 1997. The human 37-kDa laminin receptor precursor interacts with the prion protein in eukaryotic cells. Nat. Med. **3**: 1383–1388.
33) Saeki, K., Matsumoto, Y., Matsumoto, Y., and Onodera, T. 1996. Identification of a promoter region in the rat prion protein gene. Biochem. Biophys. Res. Commun. **219**:

47–52.
34) Salmona, M., Capobianco, R., Colombo, L., De Luigi, A., Rossi, G., Mangieri, M., Giaccone, G., Quaglio, E., Chiesa, R., Donati, M.B., Tagliavini, F., and Forloni, G. 2005. Role of plasminogen in propagation of scrapie. J. Virol. **79**: 11225–11230.
35) Schmitt-Ulms, G., Legname, G., Baldwin, M.A., Ball, H.L., Bradon, N., Bosque, P.J., Crossin, K.L., Edelman, G.M., DeArmond, S.J., Cohen, F.E., and Prusiner, S.B. 2001. Binding of neural cell adhesion molecules (N-CAMs) to the cellular prion protein. J. Mol. Biol. **314**: 1209–1225.
36) Stahl, N., Borchelt, D.R., and Prusiner, S.B. 1990. Differential release of cellular and scrapie prion proteins from cellular membranes by phosphatidylinositol-specific phospholipase C. Biochemistry **29**: 5405–5412.
37) Taraboulos, A., Raeber, A.J., Borchelt, D.R., Serban, D., and Prusiner, S.B. 1992. Synthesis and trafficking of prion proteins in cultured cells. Mol. Biol. Cell **3**: 851–863.
38) Taraboulos, A., Scott, M., Semenov, A., Avrahami, D., Laszlo, L., and Prusiner, S.B. 1995. Cholesterol depletion and modification of COOH-terminal targeting sequence of the prion protein inhibit formation of the scrapie isoform. J. Cell Biol. **129**: 121–132.
39) Taraboulos, A., Serban, D., and Prusiner, S.B. 1990. Scrapie prion proteins accumulate in the cytoplasm of persistently infected cultured cells. J. Cell Biol. **110**: 2117–2132.
40) Telling, G.C., Scott, M., Mastrianni, J., Gabizon, R., Torchia, M., Cohen, F.E., DeArmond, S.J., and Prusiner, S.B. 1995. Prion propagation in mice expressing human and chimeric PrP transgenes implicates the interaction of cellular PrP with another protein. Cell **83**: 79–90.
41) Vey, M., Pilkuhn, S., Wille, H., Nixon, R., DeArmond, S.J., Smart, E.J., Anderson, R.G., Taraboulos, A., and Prusiner, S.B. 1996. Subcellular colocalization of the cellular and scrapie prion proteins in caveolae-like membranous domains. Proc. Natl. Acad. Sci. U.S.A. **93**: 14945–14949.
42) Yadavalli, R., Guttmann, R.P., Seward, T., Centers, A.P., Williamson, R.A., and Telling, G.C. 2004. Calpain-dependent endoproteolytic cleavage of PrPSc modulates scrapie prion propagation. J. Biol. Chem. **279**: 21948–21956.

JOURNAL OF VIROLOGY, Dec. 2007, p. 12889–12898 Vol. 81, No. 23
0022-538X/07/$08.00+0 doi:10.1128/JVI.01563-07

Orally Administered Amyloidophilic Compound Is Effective in Prolonging the Incubation Periods of Animals Cerebrally Infected with Prion Diseases in a Prion Strain-Dependent Manner▽

Yuri Kawasaki,[1] Keiichi Kawagoe,[2] Chun-jen Chen,[2] Kenta Teruya,[1] Yuji Sakasegawa,[1] and Katsumi Doh-ura[1]*

Department of Prion Research, Tohoku University Graduate School of Medicine, Sendai, Japan,[1] and Tokyo R & D Center, Daiichi Pharmaceutical Co., Ltd., Tokyo, Japan[2]

Received 18 July 2007/Accepted 4 September 2007

The establishment of effective therapeutic interventions for prion diseases is necessary. We report on a newly developed amyloidophilic compound that displays therapeutic efficacy when administered orally. This compound inhibited abnormal prion protein formation in prion-infected neuroblastoma cells in a prion strain-dependent manner: effectively for RML prion and marginally for 22L prion and Fukuoka-1 prion. When the highest dose (0.2% [wt/wt] in feed) was given orally to cerebrally RML prion-inoculated mice from inoculation until the terminal stage of disease, it extended the incubation periods by 2.3 times compared to the control. The compound exerted therapeutic efficacy in a prion strain-dependent manner such as that observed in the cell culture study: most effective for RML prion, less effective for 22L prion or Fukuoka-1 prion, and marginally effective for 263K prion. Its effectiveness depended on an earlier start of administration. The glycoform pattern of the abnormal prion protein in the treated mice was modified and showed predominance of the diglycosylated form, which resembled that of 263K prion, suggesting that diglycosylated forms of abnormal prion protein might be least sensitive or resistant to the compound. The mechanism of the prion strain-dependent effectiveness needs to be elucidated and managed. Nevertheless, the identification of an orally available amyloidophilic chemical encourages the pursuit of chemotherapy for prion diseases.

Transmissible spongiform encephalopathies, or prion diseases, are a group of fatal neurodegenerative disorders that include Creutzfeldt-Jakob disease (CJD) and Gerstmann-Sträussler-Scheinker syndrome (GSS) in humans and scrapie, bovine spongiform encephalopathy, and chronic wasting disease in animals. These disorders are characterized by accumulation in the brain of an abnormal isoform of prion protein (PrP), which is a main component of the pathogen, prion, or a pathogen itself and which is rich in beta-sheet structure and resistant to digestion with proteinase K (24). Recent outbreaks of variant CJD and iatrogenic CJD through use of cadaveric growth hormone or dura grafts in younger people have necessitated the development of suitable therapies.

Caughey and colleagues first found Congo red and sulfated glycans to inhibit abnormal PrP formation in vitro (5, 6), although Congo red was much earlier described as a staining device for prion amyloid rods (23). Since the discovery of the therapeutic activity of Congo red, amyloidophilic compounds such as amyloid dye derivatives and glucoseaminoglycan mimetics have been noted as one class of possible therapeutic candidates for prion diseases (4, 32). Recently, the most advanced progress with amyloidophilic compounds, which have an excellent ability to permeate through the blood-brain barrier, has been made in the field of diagnosis of Alzheimer's disease. Some amyloidophilic compounds are developed as imaging probes to visualize amyloid deposits in the brains of Alzheimer's disease patients using positron emission tomography or single-photon emission computed tomography technology (3). Some of these chemicals are also useful to visualize abnormal PrP amyloids of some types of prion diseases in the brain (2, 14, 15, 28, 30).

We previously reported that some of these amyloid-imaging probes are effective as antiprion compounds and prolong the incubation periods of animals cerebrally infected with prion disease (14). We also reported that a new class of amyloidophilic chemicals, styrylbenzoazole derivatives, which have better penetration through the blood-brain barrier and which show more discrete labeling of amyloid deposition in brain tissues affected by either Alzheimer's disease or prion diseases, are effective as antiprion chemicals (15, 19). However, the efficacy of these amyloidophilic compounds, intravenously administered weekly, was not remarkable but was rather limited. In addition, their effectiveness was suggested to be prion strain dependent, but this was not fully evaluated because of the limited availability of the compounds in quantity and dosing route. It can be assumed that elevated brain chemical levels are necessary for a compound's efficacy. Therefore, a multiple-dosing regimen, which causes more sustained elevation in brain chemical levels, might be preferable to a single weekly dosing. In this study, to ascertain undefined benefits and limitations of amyloidophilic compounds as therapeutic drug candidates for prion diseases, a new class of amyloidophilic compounds which have no similarity in chemical structure with previously reported antiprion compounds was synthesized and tested for either antiprion activity in vitro or therapeutic efficacy in vivo when administered orally as a mixture with feed.

* Corresponding author. Mailing address: Department of Prion Research, Tohoku University Graduate School of Medicine, 2-1 Seiryo-cho, Aoba-ku, Sendai, Miyagi 980-8575, Japan. Phone: 81-22-717-8232. Fax: 81-22-717-7656. E-mail: doh-ura@mail.tains.tohoku.ac.jp.

▽ Published ahead of print on 19 September 2007.

TABLE 1. Tested compounds and their inhibition of abnormal PrP formation in ScN2a cells

Compound	Chemical structure	Mol wt	Octanol-water distribution coefficient[a] (log $D_{6.8}$)	Inhibition of abnormal PrP (approximate EC_{50}, nM)[b]	Maximum tolerance dose[c] (μM)
cpd-B	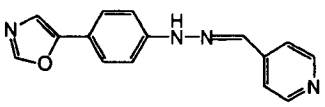	264	4.1	0.06	>10
cpd-D1	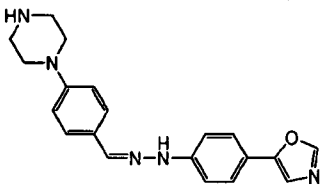	347	2.2	100	>10
cpd-D2	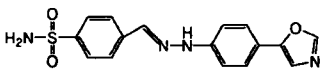	342	3.6	10	>10
cpd-D3	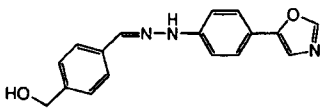	293	3.2	1	>10
cpd-D4	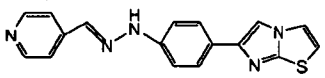	319	Not determined	1	>10
cpd-D5	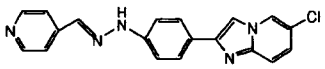	347	4.7	1	>10
cpd-D6	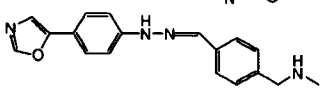	306	2.4	10	>10

[a] The distribution coefficient, a measure of a compound's hydrophilicity or hydrophobicity, was estimated using ChemAxon's calculator plugin software (Budapest, Hungary). The coefficients of medicines used for brain diseases are generally around 3.0.
[b] The approximate dose giving 50% inhibition of abnormal PrP formation relative to the control.
[c] The maximal dose that does not affect the rate of cell growth to confluence.

MATERIALS AND METHODS

Chemicals and experimental models. Test compounds were synthesized at the Tokyo R & D Center of Daiichi Pharmaceutical Co., Ltd. (Tokyo, Japan). The structures of the compounds are shown in Table 1. The compounds were dissolved in 100% dimethyl sulfoxide using ultrasonication and stored at −30°C until use.

Cultured cells were grown in Opti-MEM (Invitrogen Corp., Carlsbad, CA) supplemented with 10% fetal calf serum. As cellular models for the screening of antiprion compounds, either mouse neuroblastoma cells (N2a cells) or N2a cells with fivefold PrP overexpression (N2a-58 cells) which were persistently infected with a distinct prion strain were used, as follows: N2a cells infected with RML scrapie prion (ScN2a cells) (25), N2a cells with 22L scrapie prion (N167 cells), N2a-58 cells with RML scrapie prion (N002 or Ch2 cells), or N2a-58 cells with Fukuoka-1 GSS prion (F3 cells) (15). The Ch2 cells are a subclone of N002 cells.

Five-week-old Tga20 mice overexpressing murine PrP (11) or Tg7 mice overexpressing hamster PrP (26) were used as animal disease models after intracerebral infection with 20 μl of 1% (wt/vol) brain homogenate of RML prion, 22L prion, or Fukuoka-1 prion for Tga20 mice or 263K scrapie prion for Tg7 mice. Five-week-old ICR mice and Syrian hamsters were also used after they were infected intracerebrally with 20 μl of 1% (wt/vol) brain homogenate of RML prion or 40 μl of 1% (wt/vol) brain homogenate of 263K prion, respectively. Each animal was maintained under deep ether anesthesia for minimum distress during intracerebral inoculation. Permission for the animal study was obtained from the Animal Experiment Committee of Tohoku University, Japan.

In vitro PrP imaging. Autopsy-diagnosed brain samples from cases of GSS, which were kindly provided by Toru Iwaki from the Department of Neuropathology, Kyushu University, Japan, were used. After fixation in 10% buffered formalin for 2 weeks, the sample was immersed in 98% formic acid for reduction of prion infectivity, embedded in paraffin, and cut into 7-mm-thick sections. For neuropathological staining, deparaffinized sections were immersed in 1% Sudan black solution to quench tissue autofluorescence. They were then incubated for 30 min in 1 mM solution of compound B (cpd-B), rinsed with distilled water, and examined under a fluorescence microscope (DMRXA; Leica Microsystems GmbH, Wetzlar, Germany) using a fluorescein isothiocyanate filter set.

For comparison, each section was subsequently immunostained for PrP as described in a previous study (7). Briefly, the sections were treated with a hydrolytic autoclave and incubated with a rabbit primary antibody, anti-PrP-C, which was raised against a mouse PrP fragment consisting of amino acids 214 to 228 (1:200; Immuno-Biological Laboratories Co. Ltd., Gunma, Japan), followed by incubation with EnVision+System horseradish peroxidase labeling polymer (Dako, Glostrup, Denmark). The reaction product was developed with 3,3'-diaminobenzidine tetrahydrochloride solution and counterstained with hematoxylin.

In vitro treatment in cell cultures. Antiprion activity was evaluated by assaying the content of protease-resistant PrP (PrPres) in the cellular models, as described in earlier studies (6, 8, 18). Briefly, test compounds were added at the designated concentrations when cells were passaged at 10% confluence, while maintaining the final concentration of dimethyl sulfoxide in the medium at less than 0.5%. The cells were allowed to grow to confluence and were lysed with lysis buffer (0.5% sodium deoxycholate, 0.5% Nonidet P-40, phosphate-buffered saline [PBS]). For analysis of PrPres, samples were digested using 10 μg/ml proteinase K for 30 min at 37°C; the digestion was stopped using 1 mM phenylmethylsulfonyl fluoride. The samples were centrifuged at 100,000 × *g* for 30 min, and then pellets were resuspended in 1× sample loading buffer and boiled for 5 min. For analysis of the total level of cellular PrP in N2a cells treated with a test compound, cell lysates were mixed directly with one-quarter volume of 5× sample loading buffer and boiled for 5 min.

The samples were analyzed by immunoblotting. They were separated by electrophoresis on a 15% Tris-glycine–sodium dodecyl sulfate-polyacrylamide gel and electroblotted onto a polyvinylidene difluoride filter. The PrP was detected

using a monoclonal antibody, SAF83 (1:5000; SPI-Bio, Massy, France), followed by an alkaline phosphatase-conjugated goat anti-mouse antibody (1:20,000; Promega Corp., Madison, WI). Immunoreactivity was visualized using a CDP-Star detection reagent (Amersham, Piscataway, NJ). More than three independent assays were performed in each experiment.

The cell surface level of cellular PrP was assayed using flow cytometry, as described previously (10). Briefly, N2a cells dispersed by treatment with 0.1% collagenase (Wako Pure Chemical Industries Ltd., Osaka, Japan) were washed with ice-cold 0.5% fetal calf serum in PBS and incubated with SAF83 (1:500) or isotype-matched control immunoglobulin G1 for 20 min on ice. Cells were washed with 0.5% fetal calf serum in PBS and incubated with goat F(ab')2 fragment anti-mouse immunoglobulin G (heavy plus light chain)-phycoerythrin (1:100) (Beckman Coulter Inc., CA) for 20 min on ice. After washing, cells were analyzed using an EPICS XL-ADC flow cytometer (Beckman Coulter Inc., CA).

Pharmacokinetic studies. Brain cpd-B levels in the animals were assayed as described previously (20) after a 1-week feeding with 0.2% cpd-B ad libitum. All animals were sacrificed at 9:00 a.m. of day 8 by excision of the carotid artery under deep ether anesthesia to remove as much blood as possible, and the brain was collected, rinsed with saline, and weighed. Because preliminary studies found no significant difference in the data for perfused brains and nonperfused brains, the brain was not perfused with saline to remove residual blood. The brain was homogenized with 2 ml of 100% methanol for mouse brain or 4 ml for hamster brain. After centrifugation of the homogenate at 800 × *g* for 10 min, the supernatant was diluted with 9 volumes of 20 mM phosphate buffer, pH 6.5 (PB), and then filtered to obtain the sample for analysis. The sample was then applied to a conditioned C_{18} solid-phase extraction cartridge. The compound was eluted with methanol and was diluted with an equal volume of PB. The compound then was separated by high-performance liquid chromatography using a reversed-phase column (C_4, 4.6 × 150 mm; Phenomenex Inc., Torrance, CA). The compound was detected using a UV detector at 285 nm, and the dose of cpd-B per gram of brain tissue was determined.

The kinetics of brain uptake and washout of cpd-B were also investigated as described previously (20). The compound was solubilized in 5% Tween 80 in ethanol and then prepared as a 0.2-mg/ml solution containing 5% Tween 80 and 5% ethanol in saline. The compound at a dose of 1.0 mg/kg of body weight was administered intravenously to ICR mice under ether anesthesia. Both Tween 80 and ethanol are FDA-approved solubilizers of lipophilic medicinal chemicals. At the dose used in the study, neither solubilizer has been reported to cause any toxicity or to affect the pharmacokinetics. At 2 min or 30 min after injection, the blood was collected from the heart using heparin, and then the brain was obtained as described above. The blood plasma was mixed with 3 volumes of acetonitrile and centrifuged at 10,000 × *g* for 5 min. The supernatant was mixed with the same volume of PB and subsequently filtered to obtain the plasma sample for analysis. The preparation for the brain sample for analysis and the assay of the samples were performed as described above. The percentage of the injected dose per gram of tissue or fluid was used as a measure of the brain or plasma level of the compound.

In vivo treatment in animal models. In experimental animals that had been infected intracerebrally with a prion pathogen, cpd-B was given orally ad libitum as a mixture with powder feed at doses of 0.1%, 0.13%, 0.2%, and 0.33% by weight in the feed, corresponding, respectively, to ca. 150 mg/kg of body weight/day, ca. 225 mg/kg of body weight/day, ca. 300 mg/kg of body weight/day, and ca. 500 mg/kg of body weight/day in Tga20 mice, as each mouse consumed an average of 3.75 g of the feed per day. The animals were monitored every day until the terminal stage of disease; the incubation period, which was defined in the present study as the length of time from inoculation to the terminal stage of disease, was determined.

Pathological and infectivity assays. The right brain hemispheres of the mice were fixed using 10% buffered formalin and then embedded in paraffin. Three-micrometer-thick sections of the coronal slice sited at around one-third of the distance from the interaural line to the bregma line were dewaxed and immunostained using an anti-PrP-C antibody, as described above, or an antibody against glial fibrillary acidic protein (1:5,000; Dako, Glostrup, Denmark), as described in a previous study (9).

For detection of PrPres by immunoblotting, the left brain hemisphere was homogenized with 9 volumes of lysis buffer; after low-speed centrifugation, the supernatant was treated with 50 μg/ml proteinase K for 30 min at 37°C. An aliquot corresponding to 0.13 mg of brain tissue for PrPres assay or 0.83 μg of brain tissue for total PrP assay was electrophoresed on a 13.5% Tris-glycine–sodium dodecyl sulfate-polyacrylamide gel and analyzed by immunoblotting as described above.

For the infectivity assay, the left brain hemisphere was homogenized with PBS to produce a 10% brain homogenate. Serially diluted homogenate samples for assay were produced by diluting the brain homogenate serially with 10% brain homogenate of noninfected mice fed with 0.2% cpd-B for 1 month. A 20-μl aliquot of each sample was then inoculated intracerebrally into each of the Tga20 mice. Incubation times were assayed as described above.

Statistical analysis. Statistical significance was analyzed using the Kruskal-Wallis test followed by Scheffè's *F* test for multiple comparisons. Correlation analysis was performed using Spearman's rank correlation coefficient method. The regression coefficient was determined using simple linear regression analysis. The survival rate was calculated using the Kaplan-Meier method; its significance was evaluated using the log rank method.

RESULTS

Antiprion activity in vitro. The antiprion activities of newly synthesized compounds were investigated using ScN2a cells, which are N2a cells that are persistently infected with RML scrapie prion and are commonly used for drug screening. At a half-maximum effective concentration (EC_{50}) of about 60 pM, cpd-B inhibited PrPres formation (Table 1 and Fig. 1A). Other related compounds were also potent within a nontoxic dose range of up to 10 μM.

To investigate whether the efficacies of the compounds depend on the pathogen strain, cpd-B was tested in four other cell lines that had been infected individually with distinct prion strains. As shown in Fig. 1A, cpd-B was effective only in N002 (EC_{50}, 320 nM) and Ch2 (EC_{50}, 300 nM), both of which are N2a-58 cells infected with RML prion. However, the inhibitory activity in these cells was not as strong as that in ScN2a cells, which are derived from N2a cells expressing one-fifth of the normal PrP molecules of N2a-58 cells. In contrast, cpd-B was ineffective in both N167 cells (N2a cells infected with 22L scrapie prion) and F3 cells (N2a-58 cells infected with Fukuoka-1 GSS prion) at a dose of less than 10 μM. However, at a dose of 10 μM, a marginal reduction of the PrPres signals was observed in both cells. At a dose of greater than 10 μM, cell toxicity was observed. The results suggest that cpd-B exerts an inhibitory activity on PrPres formation in a prion strain-dependent manner: more effectively for RML prion and marginally for 22L prion or Fukuoka-1 prion.

The inhibition mechanism included no alteration of either the total or the cell surface level of normal PrP, as demonstrated in noninfected N2a cells treated with 1 μM cpd-B, using either immunoblot analysis of the cell lysate without protease digestion or flow cytometry analysis of the cell surface PrP (Fig. 1B and C). In addition, cpd-B did not facilitate the digestion of abnormal PrP by proteinase K, nor did it interfere with immunodetection, because PrPres signals were not modified after cpd-B was mixed and incubated with a cell lysate of nontreated ScN2a cells before proteinase K digestion (data not shown).

Pharmacological properties. Abnormal PrP amyloid imaging by cpd-B was performed on brain sections of GSS cases to examine the amyloidophilic properties of cpd-B. The compound bound to and fluorescently labeled most of the PrP plaques in cerebellar cortices of GSS cases (Fig. 1D). Background staining was barely observed after rinsing off the excess compound. Immunohistochemical analysis of PrP revealed that the compound achieved high-specificity labeling. The compound displayed no signal in control sections without amyloid lesions (data not shown).

Next, to examine the brain accessibility of cpd-B when administered orally, brain levels of cpd-B in the experimental

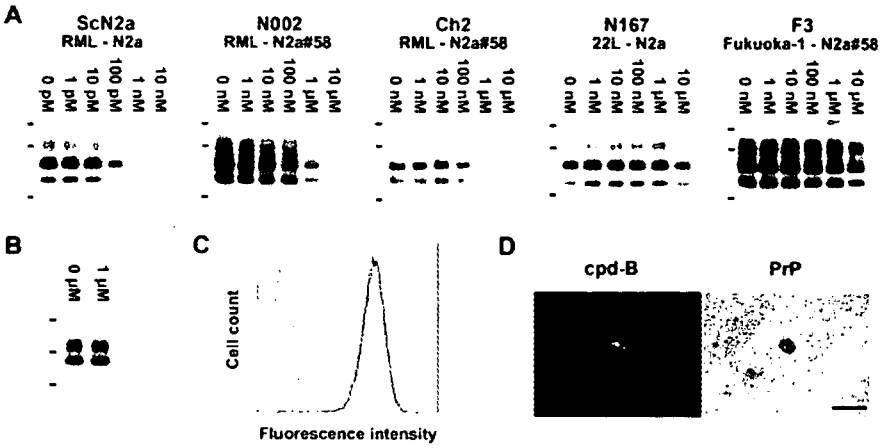

FIG. 1. cpd-B effects on prion-infected and noninfected cells and its amyloidophilic property. (A) Immunoblot analyses of PrPres formation in various prion-infected cells treated with the indicated concentrations of cpd-B. N2a-58 (N2a#58) is a stable transformant of N2a and expresses five-times-higher levels of PrP than N2a. Ch2 is a subclone of N002. The bars on the left are molecular size markers for 41, 32, and 18 kDa. (B) Immunoblot analysis of total normal PrP in noninfected N2a cells treated with cpd-B. Molecular size markers on the left are 47, 32, and 25 kDa. (C) Flow cytometric analysis of cell surface-normal PrP in noninfected N2a cells treated with 1 μM cpd-B. The solid and broken lines, respectively, indicate cpd-B-treated cells and nontreated cells. Gray line peaks on the left show their respective controls, using isotype immunoglobulin as a first antibody. (D) Imaging of abnormal PrP plaques in the brain tissue by cpd-B. Abnormal PrP deposition in a cerebellar tissue from a case of GSS was fluorescently labeled with cpd-B and subsequently immunostained with an anti-PrP antibody. Bar, 50 μm.

animals used in the study were assayed after the animals were fed ad libitum with 0.2% cpd-B-containing feed for 1 week. The brain level of cpd-B was 39.16 ± 22.15 nmol/g brain tissue in Tga20 mice (n = 4), 26.04 ± 12.50 nmol/g brain tissue in ICR mice (n = 4), and 22.94 ± 7.64 nmol/g brain tissue in Tg7 mice (n = 4). Syrian hamsters, however, showed a lower level, 7.26 ± 2.47 nmol/g brain tissue (n = 4). A considerable amount of cpd-B was detected in the brains of all experimental animals; no significant difference in the brain cpd-B levels was found among the types of the mice.

Further study of the pharmacokinetics of cpd-B in the blood and the brain was performed with ICR mice after cpd-B was injected into the tail vein. The percentage of the injected dose per gram of tissue or fluid was determined. The brain uptake level of cpd-B at 2 min after intravenous injection was 8.01% ± 1.27% of the injected dose/g tissue, whereas the blood plasma level was 2.92% ± 1.00%/g fluid. Consequently, the ratio of the cpd-B concentration in the brain to that in the blood plasma is 2.7:1, indicating that cpd-B is equal to the best brain-entering amyloidophilic chemicals previously identified (15). On the other hand, both the brain level and the blood plasma level of cpd-B at 30 min after the intravenous injection were below the measurable level of 50 pM, which indicates that cpd-B is very rapidly washed out from the brain and blood.

Regarding toxicity of cpd-B, body weight losses of about 16% in Tga20 mice and about 5% in Tg7 mice were observed after cpd-B was given orally ad libitum for 1 week at a dose of 0.33% weight in feed, which corresponds to ca. 500 mg/kg of body weight/day. Other doses of cpd-B tested in this study produced no apparent toxic effects in the experimental animals used.

Therapeutic efficacy in vivo. The therapeutic activity of cpd-B in vivo was assayed in murine PrP-overexpressing Tga20 mice that had been cerebrally infected with RML scrapie prion. The nontreated infected mice started exhibiting abnormal clinical signs such as staggering, rotating, irritation, and motionlessness at about 2 months after the infection; the mice then wasted into the terminal stage of disease in a week. Treatment by feeding cpd-B-containing feed ad libitum was initiated immediately after the infection and continued until the terminal stage of disease. The cpd-B-treated mice did not exhibit such abnormal signs as described above and wasted gradually into the terminal stage of disease. As shown in Fig. 2A, oral cpd-B treatment significantly prolonged the incubation periods of infected Tga20 mice in a dose-dependent manner; these were 68.5 ± 5.9 days in the nontreated control mice, 108.0 ± 2.8 days in the mice treated with 0.1% cpd-B feed, 120.5 ± 10.7 days in the mice with 0.13% cpd-B feed, and 154.3 ± 19.9 days in the mice with 0.2% cpd-B feed. Therefore, oral cpd-B treatment at the highest dose produced a 2.3-fold extension of the incubation periods of the mice. Statistical analyses demonstrated a significant linear correlation between the incubation periods and the cpd-B doses (r = 0.95; P < 0.01); the correlation equation was $y = 426.37x + 66.93$ (y, incubation period [days]; x, cpd-B dose [percentage in feed]), and the correlation coefficient was 0.89 (P < 0.01).

In our previous studies, the effectiveness of amyloidophilic chemicals in the extension of incubation periods of infected animals was observed only in Tga20 mice infected with RML prion (14, 15). ICR mice were then examined for the therapeutic efficacy of oral cpd-B treatment to investigate whether effectiveness of amyloidophilic compounds is restricted only to Tga20 mice. Nontreated control ICR mice that had been cerebrally infected with RML prion were in the terminal stage of disease at 154.2 ± 18.4 days postinfection, whereas the mice treated with 0.2% cpd-B feed lived significantly longer (P < 0.01). Even though the oral cpd-B treatment was discontinued at day 187 postinfection when the last of the nontreated animals reached the terminal stage of disease, more than half of the treated mice survived to day 270 postinfection (Fig. 2B).

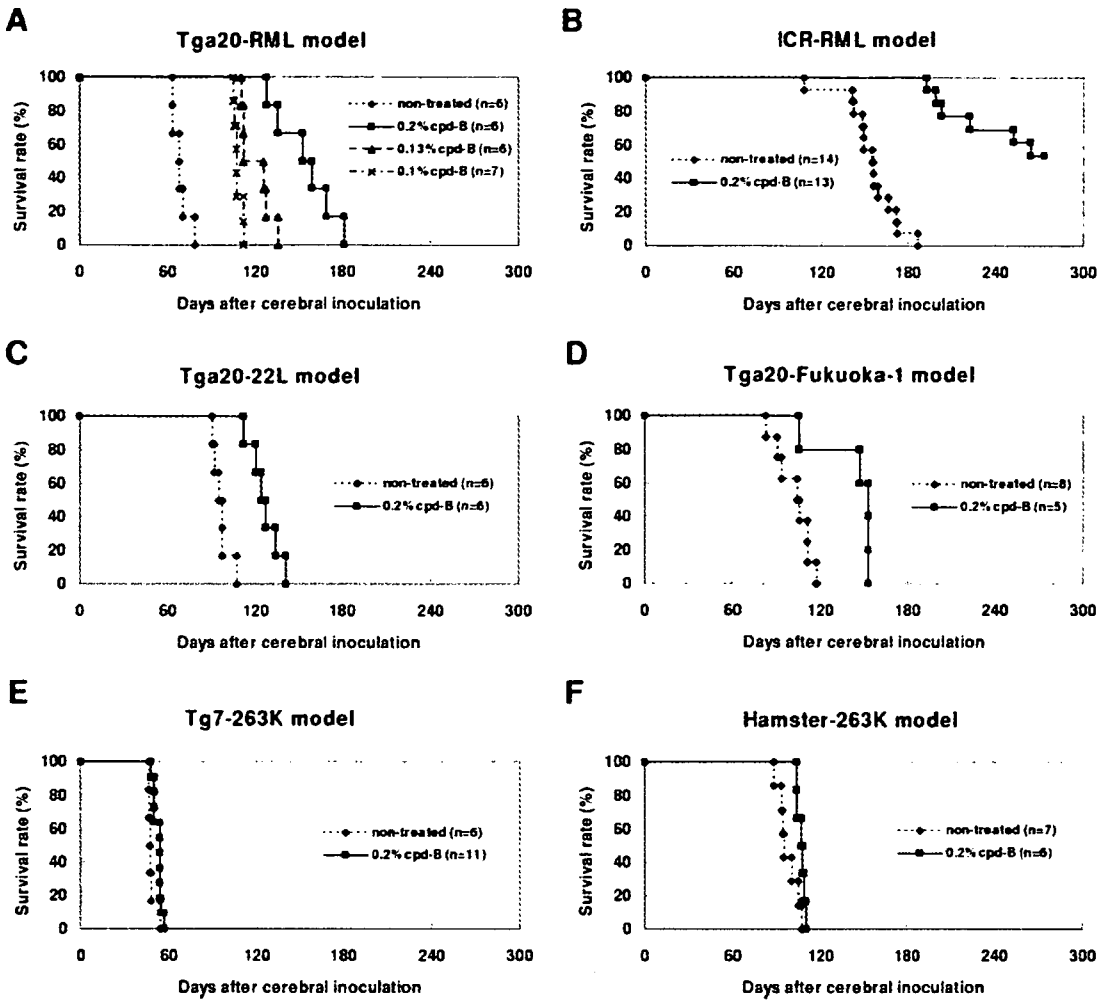

FIG. 2. Effects of orally administered cpd-B on animals cerebrally infected with prion diseases. cpd-B was given orally in a mixed form with powder feed ad libitum throughout the incubation periods in all animal disease models except the ICR-RML model, in which oral cdp-B treatment was discontinued at the time when the last of the nontreated animals reached the terminal stage of disease. In this study, the incubation periods are defined as the periods from the cerebral infection to the terminal stage of disease. Survival rates were calculated using the incubation periods and are plotted using the Kaplan-Meier method.

Next, the therapeutic efficacy of oral cpd-B treatment against other prion strains was investigated. The cpd-B treatment significantly prolonged the incubation periods of Tga20 mice that had been cerebrally infected with 22L scrapie prion ($P < 0.01$); these were 96.3 ± 5.9 days in the nontreated control mice and 126.3 ± 10.3 days in the mice treated with 0.2% cpd-B feed, indicating a 1.3-fold extension of the incubation period (Fig. 2C). Control mice started exhibiting distinguished opisthotonus with head rotating a week before the terminal stage of disease, whereas cpd-B treated mice showed no such clinical sign, even in the terminal stage.

cpd-B was also effective against Fukuoka-1 GSS prion. Cerebrally infected Tga20 mice lived significantly longer with oral cpd-B treatment ($P < 0.05$), i.e., 101.6 ± 12.1 days for the nontreated control mice and 142.2 ± 21.0 days for the mice treated with 0.2% cpd-B feed, indicating a 1.4-fold extension of the incubation period (Fig. 2D). Staggering was observed as an initial clinical sign in the control mice more than 1 week before the terminal stage of disease, although this clinical sign was not seen in the cpd-B treated mice.

In contrast to the case for these prion strains, the efficacy of oral cpd-B treatment was very marginal for 263K scrapie prion when Tg7 mice expressing hamster PrP were used as the host (Fig. 2E). The incubation periods of the cpd-B-treated mice (52.7 ± 2.8 days) were significantly but very marginally longer than those of the nontreated mice (48.0 ± 3.0 days) ($P < 0.05$). This prion is a hamster-adapted scrapie prion strain; Syrian hamsters were used as the host to examine whether the marginal efficacy of oral cpd-B treatment is attributable chiefly to the host Tg7 mouse or to the pathogen strain 263K prion. As observed in Tg7 mice, hamsters treated with 0.2% cpd-B feed also exhibited a marginal increase in the incubation period compared to that of the nontreated control hamsters that had been cerebrally infected with 263K prion ($P < 0.05$): 107.0 ± 2.5 days in the cpd-B treated hamsters and 97.4 ± 6.9 days in the non-

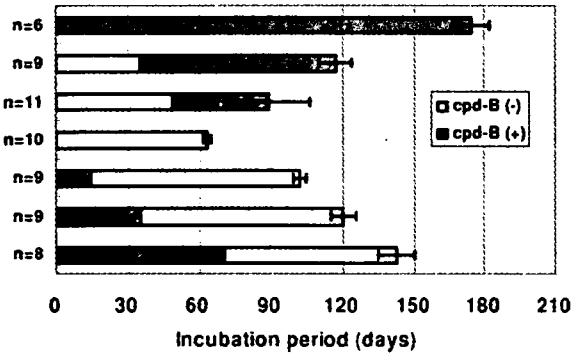

FIG. 3. cpd-B effects throughout various timings and durations of oral administration. Tga20 mice cerebrally infected with RML prion were treated with 0.2% cpd-B feed at different times and for different durations, and the incubation periods were assayed. Open bars indicate the durations of no treatment [cpd-B (−)]. Shaded bars indicate the durations of oral cpd-B treatment [cpd-B (+)].

treated hamsters (Fig. 2F). These results indicate that oral cpd-B treatment is not as effective for 263K prion.

Timing and duration of dosing. The effectiveness of cpd-B at various timings and durations of oral administration was analyzed in Tga20 mice that had been cerebrally infected with RML prion (Fig. 3). The incubation periods of the nontreated mice were 63.0 ± 1.8 days, whereas the incubation periods of the mice treated with 0.2% cpd-B feed were inversely correlated with the postinfection durations to the commencement of cpd-B treatment ($r = -0.79$; $P < 0.01$): 174.5 ± 7.6 days when started at day 0 postinfection, 117.2 ± 7.0 days when started at day 35 postinfection, and 88.7 ± 17.3 days when started at day 49 postinfection. On the other hand, the incubation periods of the mice treated with 0.2% cpd-B feed were also correlated with the durations of cpd-B treatment which started immediately after cerebral infection ($r = 0.95$, $P < 0.01$): 102.1 ± 2.9 days when treated for 14 days from the infection, 120.2 ± 5.2 days when treated for 35 days from the infection, and 142.5 ± 7.8 days when treated for 70 days from the infection. In addition, when the cpd-B treatment was discontinued during early disease stages, the remaining incubation times were longer than that of the control mice.

Pathological evaluation. The PrPres content in the brains of cpd-B-treated mice was analyzed sequentially by immunoblotting and compared with that in the nontreated control mice (Fig. 4A). The PrPres signals in the nontreated mice were very strong at the terminal stage of disease (day 63 postinfection). In contrast, in the mice treated with 0.1% cpd-B feed from the start of infection, PrPres signals were faint at day 63 postinfection and distinct at the terminal stage of disease (day 108 postinfection). However, the PrPres signals at the terminal stage of disease did not reach the high level shown by the nontreated control mice at that stage. Comparison of the signal intensities of the diglycosylated PrPres form showed that 6- to 15-fold-diluted samples from the nontreated terminal mice exhibited signal intensities similar to those of undiluted or 2-fold-diluted samples from the 0.1% cpd-B-treated terminal mice (Fig. 4B). Similarly, in the mice treated with 0.2% cpd-B feed from the start of infection, PrPres signals gradually increased according to the time course after infection: no signals were detected at day 63 postinfection, distinct signals were detected at day 120, and similar or more distinct signals were detected at the terminal stage of infection (day 154 postinfection). The PrPres signal levels of the 0.2% cpd-B-treated mice at the terminal stage of disease were indistinguishable from those of the 0.1% cpd-treated mice at the terminal stage of disease.

The glycoform patterns of PrPres differed completely. As shown in Fig. 4B, when the samples were diluted and reassayed so that the signal intensities of diglycosylated PrPres forms were equalized as much as possible, the difference was much more distinct. The glycoform patterns in the nontreated mice, which were uniform in the analyzed samples, were predominantly monoglycosylated, whereas the glycoform patterns in the cpd-B-treated mice were not necessarily uniform but were always predominantly diglycosylated. This predominance of diglycosylated PrPres was also observed for 263K prion (Fig. 4C) but not for other prion strains used in this study (data not shown).

Modification in the pathology of the brains of cpd-B-treated mice was analyzed (Fig. 4D). For nontreated control mice with an incubation period of 63 days, the brain showed prominent pathological changes consisting of abnormal PrP deposition and glial cell reaction in the thalamus, although the brains of the mice treated with 0.2% cpd-B feed showed no such pathological changes at day 63 postinfection and milder levels of abnormal PrP deposition at the terminal stage of disease (day 154 postinfection). No difference was apparent in the pattern or distribution of abnormal PrP deposition in the brains between the nontreated mice and the cpd-B-treated mice.

Infectivity analysis. Infectivity levels are inversely correlated with incubation periods (24). Therefore, infectivity levels of the brains of the mice treated with 0.2% cpd-B feed were evaluated by assaying the incubation periods of animals that had been cerebrally inoculated with the brain homogenate (Table 2). The 10^2-fold-diluted brain homogenates from the cpd-B-treated mice at day 63 postinfection exhibited incubation periods similar to those of the 10^5-fold- or greater diluted brain homogenates from the nontreated mice; the 10^2-fold-diluted brain homogenates from the cpd-B-treated mice at the terminal stage of disease (day 154 postinfection) showed incubation periods similar to those of the 10^4-fold- or 10^5-fold-diluted brain homogenates from the nontreated mice. The data indicate that the brains of mice treated with 0.2% cpd-B feed had much lower infectivity levels than those of the nontreated mice at the same time point after infection and even at the terminal stage of disease. A 100-fold to 1,000-fold difference in infectivity levels was apparent between the nontreated terminal mice and the cpd-B-treated terminal mice, although a less-than-100-fold difference in PrPres levels between the two mouse groups was estimated from the immunoblot data shown in Fig. 4B. On the other hand, no inconsistency was apparent in the gaps in the infectivity levels and the PrPres levels between the cpd-B-treated mice at day 63 postinfection and those at the terminal stage of disease. The gap in infectivity levels between these two groups was around 10-fold; 10-fold dilution of the samples from the cpd-B-treated terminal mice similarly produced no signals on the immunoblot, as observed in the samples from the cpd-B-treated mice at day 63 postinfection (data not shown).

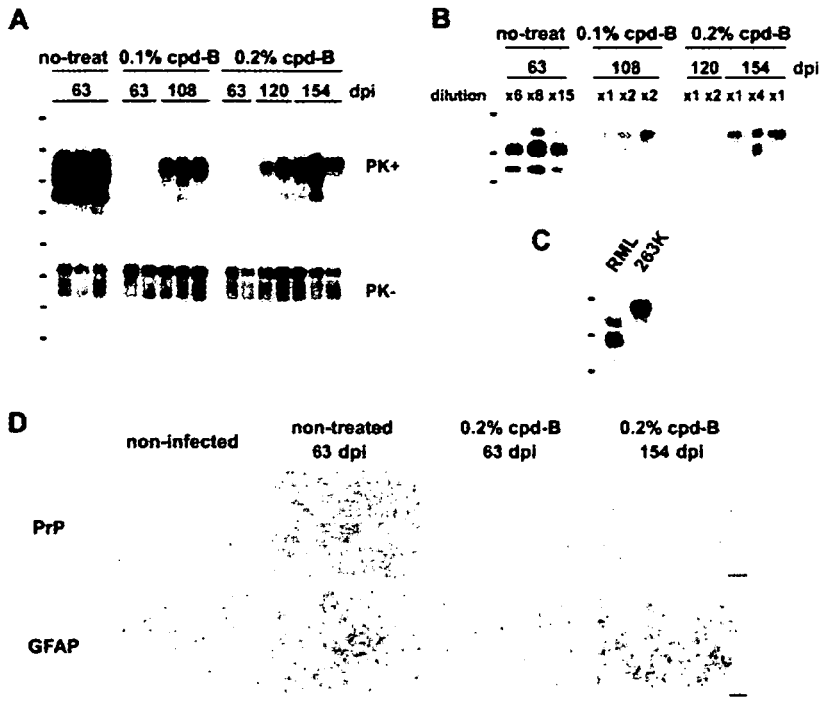

FIG. 4. Immunoblot and immunohistochemical analyses of cpd-B-treated animal brains. (A) Immunoblot analysis of PrP in the brains of nontreated mice (no-treat) or mice treated with 0.1% cpd-B feed or 0.2% cpd-B feed. Each lane represents an aliquot corresponding to 0.13 mg for PrPres (PK+) or 0.83 μg for total PrP (PK−) of brain tissue from each mouse sacrificed at a designated day after cerebral infection (dpi). Molecular size markers on the left show 47, 32, 25, and 16 kDa. (B) Immunoblot analysis of PrPres of some of the samples in panel A, which were diluted and reassayed to equalize signal intensities of the diglycosylated PrPres bands as much as possible for comparison of the signal intensity and the glycoform pattern of PrPres. Molecular size markers on the left show 32, 25, and 16 kDa. (C) Immunoblot analysis of PrPres to compare the glycoform patterns of the RML prion and the 263K prion. Analyzed samples were from an RML prion-infected mouse brain and a 263K prion-infected hamster brain. Molecular size markers on the left are the same as those in panel B. (D) Immunohistochemical analysis of abnormal PrP deposition (PrP) and neurodegenerative changes by means of astrocytic glial reaction (glial fibrillary acidic protein [GFAP]) in the brains of noninfected mice, infected but nontreated mice, and infected mice treated with 0.2% cpd-B feed. Data from each representative mouse sacrificed at a designated day after cerebral infection (dpi) are shown; every picture was taken from an almost identical area of the thalamus. The samples of 0.2% cpd-B at 63 dpi and 0.2% cpd-B at 154 dpi are from the same individual mouse as the samples in the right lane of 0.2% cpd-B 63 dpi and the rightmost lane of 0.2% cpd-B 154 dpi in panel A, respectively. Bar, 50 μm.

DISCUSSION

In this study, the newly synthesized chemical cpd-B was discovered as an orally available antiprion compound that is effective for prolonging the incubation periods of animals cerebrally infected with prion diseases. This compound has no similarity in chemical structure to previously reported antiprion compounds, although the compound shares the following properties with antiprion amyloidophilic chemicals we previously reported, such as (*trans*, *trans*)-1-bromo-2,5-bis-(3-hydroxycarbonyl-4-hydroxy)styrylbenzene and styrylbenzoazole chemicals: binding to PrP amyloid plaques in the brain tissue, inhibiting abnormal PrP formation in prion-infected cells without any effect on either normal PrP expression level or protease sensitivity of abnormal PrPres, preferential antiprion effects in RML prion-infected cells rather than 22L prion-infected or Fukuoka-1 prion-infected cells, and prolonging the incubation period in the RML prion-infected Tga20 mouse model but never or only marginally in the 263K prion-infected Tg7 mouse model. The discovery of orally available cpd-B effectiveness reinforces the idea that amyloidophilic chemicals can serve as one class of antiprion drug candidates.

This study has shown that prion strains are definitely influential in the outcome of the treatment with antiprion compounds. Treatment with cpd-B was effective against all tested prion strains, but both its antiprion effectiveness in vitro and its therapeutic efficacy in vivo were consistently dependent on the prion strain. In fact, cpd-B was most effective against RML prion but less effective against 22L prion and Fukuoka-1 prion either in vitro or in vivo. In addition, its lowest effectiveness in therapeutic efficacy was demonstrated identically in either the 263K prion-infected Tg7 mouse model or the 263K prion-infected hamster model, although its effectiveness against 263K prion could not be evaluated on the same host background as that used for the other prion strains. It is unlikely that differences in the hosts used in this study are influential in the therapeutic efficacy of cpd-B treatment, because the brain chemical levels in all types of mice fed with 0.2% cpd-B for 1 week were not significantly different.

Amyloidophilic chemicals are not the only class of antiprion compound that exhibits the therapeutic efficacy in a prion strain-dependent manner. The polyene antibiotic amphotericin B is another example, but it is opposite to amyloidophilic chemicals and is specifically effective against 263K prion (1).

TABLE 2. Infectivity assays of the brains of nontreated mice or cpd-B-treated mice

Dilution	Nontreated mice (63 dpi[a])			cpd-B treated mice (63 dpi)			cpd-B treated mice (154 dpi)		
	Mouse no.	No. of diseased mice/total	Mean incubation time (days) ± SD	Mouse no.	No. of diseased mice/total	Mean incubation time (days) ± SD	Mouse no.	No. of diseased mice/total	Mean incubation time (days) ± SD
10^{-2}	cnt-1	8/8	77.4 ± 4.5	bc-1[d]	7/7	284.1 ± 54.6	bl-1	7/7	122.0 ± 14.0
				bc-2[e]	8/8	136.8 ± 19.2	bl-2[f]	7/7	92.6 ± 8.9
							bl-3	7/7	89.1 ± 4.0
10^{-3}	cnt-1	8/8	84.4 ± 6.9	bc-1[d]	0/7	>140[c]	bl-1	5/9	>140[c]
	cnt-2	6/6	75.3 ± 2.4	bc-2[e]	1/8	>140[c]	bl-2[f]	7/7	97.4 ± 9.6
	cnt-3	7/7	75.7 ± 7.4				bl-3	9/9	101.6 ± 7.4
10^{-4}	cnt-1	7/7	88.4 ± 7.3	bc-1[d]	1/8	>140[c]	bl-1	1/9	>140[c]
				bc-2[e]	1/9	>140[c]	bl-2[f]	3/7	>140[c]
							bl-3	3/7	>140[c]
10^{-5}	cnt-1	6/6	155.7 ± 55.3						
	cnt-2	7/7	105.4 ± 16.5						
	cnt-3	7/7	95.9 ± 7.1						
10^{-6}	cnt-1	1/7	>420[b]						
10^{-7}	cnt-1	3/7	>420[b]						
10^{-8}	cnt-1	1/7	>420[b]						
10^{-9}	cnt-1	2/7	>420[b]						

[a] Days after cerebral inoculation.
[b] Observed up to 420 days postinoculation.
[c] Observed up to 140 days postinoculation.
[d] Mouse for the sample in the left lane of 0.2% cpd-B at 63 dpi in Fig. 4A.
[e] Mouse for the sample in the right lane of 0.2% cpd-B at 63 dpi in Fig. 4A.
[f] Mouse for the sample of the rightmost lane of 0.2% cpd-B at 154 dpi in Fig. 4A.

Either variation in strain-specific PrP conformational structures or variation in microenvironments facilitating PrP conformational changes might be involved in the mechanism of prion strain-dependent efficacy. The results of this study showed that prions producing predominantly diglycosylated PrPres molecules were least sensitive or resistant to cpd-B treatment, which suggests that either the conformational structure responsible for PrPres or the diglycosylation moieties might affect the interaction of the compound with abnormal PrP molecules, although this inference must be examined further. The findings indicate that each class of antiprion compounds must be examined using various prion strains to learn more about prion strain dependency.

Even in the terminal stage of disease, both abnormal PrP deposition levels in the brain and infectivity levels in the brain were reduced in the mice treated with cpd-B compared to the nontreated control mice. It remains unclear why this gap occurs. One possibility is that the treated mice prematurely fell into the terminal stage because of accumulated cpd-B toxicity. This inference, however, does not seem to be correct, because the noninfected mice treated with 0.2% cpd-B feed for more than 1 year showed no clinical signs and appeared healthy. Another possibility is that neuronal cells in the brain might be more vulnerable to lower levels of abnormal PrP in the presence of cpd-B or that abnormal PrP bound with cpd-B might be more toxic to the neuronal cells in the brain. However, these inferences also seem to be unlikely, because the toxicity of PrP106-126 peptide amyloid, which is reminiscent of abnormal PrP, in primary neuronal cell cultures is attenuated by the presence of cpd-B (unpublished data). Another possibility is that prion strains modified or selected from the original by the compound might multiply in the animals and cause the disease; this inference is supported by data showing that PrPres molecules with different glycoform patterns were detected in the treated mice. Further study, however, must provide evidence to support this inference. The findings indicate that life-threatening levels of either infectivity or abnormal PrP in the brain are not necessarily the same between treated animals and nontreated animals.

A large quantity of cpd-B was needed for efficacy in vivo; disease progression was not halted even though the treatment commenced immediately after the infection and continued to the terminal stage of disease. This limited effectiveness of cpd-B might be partly attributable to the pharmacological properties of its rapid washout from either the brain or the blood, because it is assumed that the compounds with better brain permeativity and longer retention in the brain might produce more beneficial results in prion-infected animals. In addition, some metabolic instability of the compound might be responsible for its limited effectiveness, especially the loss of efficacy during long-term administration. In fact, cpd-B is easily metabolized in the presence of mouse liver microsome extracts (unpublished data). Therefore, the pharmacokinetic parameters of this compound must be improved for better efficacy.

The effectiveness of cpd-B is dependent upon the timing and duration of administration; an earlier start of administration is

necessary to maximize beneficial results. Therefore, diagnostic measures in much earlier disease stages, especially presymptomatic stages, are vital to produce more beneficial outcomes. In addition, multidrug combination chemotherapy using several antiprion compounds with different actions might produce more beneficial results. This study suggests that cpd-B inhibits new formation of abnormal PrP but does not facilitate the degradation of already formed abnormal PrP, because a mixture of cpd-B with abnormal PrP did not modify the protease-resistant property of abnormal PrP. In addition, cpd-B itself has no activity to protect neuronal cells from neurotoxic insults aside from PrP amyloid (unpublished data), suggesting that cpd-B does not protect neuronal cells from neurodegenerative insults that are induced secondarily by abnormal PrP. Combinations of cpd-B with other compounds such as doxycycline, flupirtine, and simvastatin might be examples, but their efficacy must be evaluated. Doxycycline is a tetracycline antibiotic known to destabilize abnormal PrP (12). Flupirtine is a centrally acting nonopioid analgesic and protects neuronal cells from apoptotic cell death induced by toxic PrP106-126 peptide amyloid (29). It was used in clinical trials, where beneficial effects on cognitive functions in patients with CJD were proved (21). Simvastatin is a cholesterol-lowering drug known to prevent abnormal PrP formation in prion-infected cells, presumably by redistribution of normal PrP away from cholesterol-rich lipid rafts (13, 31). It prolongs survival times in prion-infected animals (16, 17).

Recently, long-term cerebroventricular administration of pentosan polysulfate (PPS), a clinical approach based on our preclinical study in rodent models of prion diseases (9), has been carried out in 26 patients with various types of diseases (27). Although its therapeutic efficacy remains to be confirmed, preliminary clinical experience indicates prolonged survival in some patients receiving long-term PPS (22, 27). Further prospective investigation of PPS administration is necessary to obtain high-quality evidence for its clinical benefits. However, this treatment has some weaknesses. One is the requirement for surgical implantation of a continuous infusion pump and an intraventricular catheter, which could become an obstacle to extension of clinical trials because of the potential risks of prion contamination in operating rooms and of operation instruments, although most developed countries now possess clearly defined and well established guidelines for safe surgical and anesthetic management of patients with prion diseases. Compared to such treatments, the treatments using orally available antiprion compounds are absolutely preferable and practical.

The compounds tested in the study were originally designed as therapeutic lead chemicals for the treatment of Alzheimer's disease. In fact, cpd-B and related chemicals are very effective in vitro in either inhibiting beta-amyloid formation or protecting neuronal cells from beta-amyloid toxicity; in addition, cpd-B has therapeutic efficacy in an Alzheimer's disease mouse model (unpublished data). Therefore, cpd-B is a therapeutic candidate not only for prion diseases but also for Alzheimer's disease. The search for and development of drugs for prion diseases reportedly do not interest pharmaceutical companies because of the limited number of patients, but the possible use of amyloidophilic chemicals as drug candidates for both prion diseases and Alzheimer's disease might attract and accelerate the development of therapeutic drugs for prion diseases.

In conclusion, our findings related to the newly synthesized amyloidophilic chemical cpd-B are encouraging, but further improvement of its safety profiles and pharmacokinetic properties is necessary before clinical application can be considered. Moreover, additional problems exist with its prion strain-dependent effectiveness and with its reduced effectiveness if administered at later disease stages.

ACKNOWLEDGMENTS

This work was supported by grants from the Japanese Ministry of Health, Labor and Welfare (H16-kokoro-024 and H19-nanji-006); the Japanese Ministry of Agriculture, Forestry and Fisheries; and the Japan Society for the Promotion of Science (A2-14207030 and B-19390234).

We thank Kayoko Motoki, Takashi Odagiri, and Tetsuya Mimura from Daiichi Pharmaceutical Co., Ltd., for synthesis of the amyloidophilic compounds tested in the study; Yuki Yamada and Hiroto Akama from Tohoku University for technical assistance; and Tetsuyuki Kitamoto and Yukitsuka Kudo from Tohoku University for helpful suggestions.

REFERENCES

1. **Adjou, K. T., J. P. Deslys, R. Demaimay, and D. Dormont.** 1997. Probing the dynamics of prion diseases with amphotericin B. Trends Microbiol. **5**:27–31.
2. **Bresjanac, M., L. M. Smid, T. D. Vovko, A. Petric, J. R. Barrio, and M. Popovic.** 2003. Molecular-imaging probe 2-(1-[6-[(2-fluoroethyl)(methyl)-amino]-2-naphthyl]ethylidene)malononitrile labels prion plaques in vitro. J. Neurosci. **23**:8029–8033.
3. **Cai, L., R. B. Innis, and V. W. Pike.** 2007. Radioligand development for PET imaging of beta-amyloid (Abeta)—current status. Curr. Med. Chem. **14**: 19–52.
4. **Cashman, N. R., and B. Caughey.** 2004. Prion diseases—close to effective therapy? Nat. Rev. Drug Discov. **3**:874–884.
5. **Caughey, B., and R. E. Race.** 1992. Potent inhibition of scrapie-associated PrP accumulation by Congo red. J. Neurochem. **59**:768–771.
6. **Caughey, B., and G. J. Raymond.** 1993. Sulfated polyanion inhibition of scrapie-associated PrP accumulation in cultured cells. J. Virol. **67**:643–650.
7. **Doh-ura, K., E. Mekada, K. Ogomori, and T. Iwaki.** 2000. Enhanced CD9 expression in the mouse and human brains infected with transmissible spongiform encephalopathies. J. Neuropathol. Exp. Neurol. **59**:774–785.
8. **Doh-Ura, K., T. Iwaki, and B. Caughey.** 2000. Lysosomotropic agents and cysteine protease inhibitors inhibit scrapie-associated prion protein accumulation. J. Virol. **74**:4894–4897.
9. **Doh-ura, K., K. Ishikawa, I. Murakami-Kubo, K. Sasaki, S. Mohri, R. Race, and T. Iwaki.** 2004. Treatment of transmissible spongiform encephalopathy by intraventricular drug infusion in animal models. J. Virol. **78**:4999–5006.
10. **Doh-Ura, K., T. Kuge, M. Uomoto, K. Nishizawa, Y. Kawasaki, and M. Iha.** 2007. Prophylactic effect of dietary seaweed fucoidan against enteral prion infection. Antimicrob. Agents Chemother. **51**:2274–2277.
11. **Fischer, M., T. Rulicke, A. Raeber, A. Sailer, M. Moser, B. Oesch, S. Brandner, A. Aguzzi, and C. Weissmann.** 1996. Prion protein (PrP) with amino-proximal deletions restoring susceptibility of PrP knockout mice to scrapie. EMBO J. **15**:1255–1264.
12. **Forloni, G., S. Iussich, T. Awan, L. Colombo, N. Angeretti, L. Girola, I. Bertani, G. Poli, M. Caramelli, M. Grazia Bruzzone, L. Farina, L. Limido, G. Rossi, G. Giaccone, J. W. Ironside, O. Bugiani, M. Salmona, and F. Tagliavini.** 2002. Tetracyclines affect prion infectivity. Proc. Natl. Acad. Sci. USA **99**:10849–10854.
13. **Gilch, S., C. Kehler, and H. M. Schatzl.** 2006. The prion protein requires cholesterol for cell surface localization. Mol. Cell Neurosci. **31**:346–353.
14. **Ishikawa, K., K. Doh-ura, Y. Kudo, N. Nishida, I. Murakami-Kubo, Y. Ando, T. Sawada, and T. Iwaki.** 2004. Amyloid imaging probes are useful for detection of prion plaques and treatment of transmissible spongiform encephalopathies. J. Gen. Virol. **85**:1785–1790.
15. **Ishikawa, K., Y. Kudo, N. Nishida, T. Suemoto, T. Sawada, T. Iwaki, and K. Doh-ura.** 2006. Styrylbenzoazole derivatives for imaging of prion plaques and treatment of transmissible spongiform encephalopathies. J. Neurochem. **99**:198–205.
16. **Kempster, S., C. Bate, and A. Williams.** 2007. Simvastatin treatment prolongs the survival of scrapie-infected mice. Neuroreport **18**:479–482.
17. **Mok, S. W., K. M. Thelen, C. Riemer, T. Bamme, S. Gultner, D. Lutjohann, and M. Baier.** 2006. Simvastatin prolongs survival times in prion infections of the central nervous system. Biochem. Biophys. Res. Commun. **348**:697–702.
18. **Murakami-Kubo, I., K. Doh-Ura, K. Ishikawa, S. Kawatake, K. Sasaki, J.**

Kira, S. Ohta, and T. Iwaki. 2004. Quinoline derivatives are therapeutic candidates for transmissible spongiform encephalopathies. J. Virol. **78**:1281–1288.

19. **Okamura, N., T. Suemoto, H. Shimadzu, M. Suzuki, T. Shiomitsu, H. Akatsu, T. Yamamoto, M. Staufenbiel, K. Yanai, H. Arai, H. Sasaki, Y. Kudo, and T. Sawada.** 2004. Styrylbenzoxazole derivatives for in vivo imaging of amyloid plaques in the brain. J. Neurosci. **24**:2535–2541.
20. **Okamura, N., T. Suemoto, S. Furumoto, M. Suzuki, H. Shimadzu, H. Akatsu, T. Yamamoto, H. Fujiwara, M. Nemoto, M. Maruyama, H. Arai, K. Yanai, T. Sawada, and Y. Kudo.** 2005. Quinoline and benzimidazole derivatives: candidate probes for in vivo imaging of tau pathology in Alzheimer's disease. J. Neurosci. **25**:10857–10862.
21. **Otto, M., L. Cepek, P. Ratzka, S. Doehlinger, I. Boekhoff, J. Wiltfang, E. Irle, G. Pergande, B. Ellers-Lenz, O. Windl, H. A. Kretzschmar, S. Poser, and H. Prange.** 2004. Efficacy of flupirtine on cognitive function in patients with CJD: a double-blind study. Neurology **62**:714–718.
22. **Parry, A., I. Baker, R. Stacey, and S. Wimalaratna.** 2007. Long term survival in a patient with variant Creutzfeldt-Jakob disease treated with intraventricular pentosan polysulphate. J. Neurol. Neurosurg. Psychiatry **78**:733–734.
23. **Prusiner, S. B., M. P. McKinley, K. A. Bowman, D. C. Bolton, P. E. Bendheim, D. F. Groth, and G. G. Glenner.** 1983. Scrapie prions aggregate to form amyloid-like birefringent rods. Cell **35**:349–358.
24. **Prusiner, S. B.** 1991. Molecular biology of prion diseases. Science **252**:1515–1522.
25. **Race, R. E., B. Caughey, K. Graham, D. Ernst, and B. Chesebro.** 1988. Analyses of frequency of infection, specific infectivity, and prion protein biosynthesis in scrapie-infected neuroblastoma cell clones. J. Virol. **62**:2845–2849.
26. **Race, R. E., S. A. Priola, R. A. Bessen, D. Ernst, J. Dockter, G. F. Rall, L. Mucke, B. Chesebro, and M. B. Oldstone.** 1995. Neuron-specific expression of a hamster prion protein minigene in transgenic mice induces susceptibility to hamster scrapie agent. Neuron **15**:1183–1191.
27. **Rainov, N. G., Y. Tsuboi, P. Krolak-Salmon, A. Vighetto, and K. Doh-Ura.** 2007. Experimental treatments for human transmissible spongiform encephalopathies: is there a role for pentosan polysulfate? Expert Opin. Biol. Ther. **7**:713–726.
28. **Sadowski, M., J. Pankiewicz, H. Scholtzova, J. Tsai, Y. Li, R. I. Carp, H. C. Meeker, P. Gambetti, M. Debnath, C. A. Mathis, L. Shao, W. B. Gan, W. E. Klunk, and T. Wisniewski.** 2004. Targeting prion amyloid deposits in vivo. J. Neuropathol. Exp. Neurol. **63**:775–784.
29. **Schroder, H. C., and W. E. Muller.** 2002. Neuroprotective effect of flupirtine in prion disease. Drugs Today **38**:49–58.
30. **Smid, L. M., T. D. Vovko, M. Popovic, A. Petric, V. Kepe, J. R. Barrio, G. Vidmar, and M. Bresjanac.** 2006. The 2,6-disubstituted naphthalene derivative FDDNP labeling reliably predicts Congo red birefringence of protein deposits in brain sections of selected human neurodegenerative diseases. Brain Pathol. **16**:124–130.
31. **Taraboulos, A., M. Scott, A. Semenov, D. Avrahami, L. Laszlo, and S. B. Prusiner.** 1995. Cholesterol depletion and modification of COOH-terminal targeting sequence of the prion protein inhibit formation of the scrapie isoform. J. Cell Biol. **129**:121–132.
32. **Trevitt, C. R., and J. Collinge.** 2006. A systematic review of prion therapeutics in experimental models. Brain **129**:2241–2265.

FULL PAPER *Public Health*

Distribution of the Lingual Tonsils of Cattle Designated as Specified Risk Materials

Keiko KATO[1)] and Yasushi SAWADA[2)]

[1)]*Animal Care and Consultation Center, Bureau of Social Welfare and Public Health, Tokyo Metropolitan Government, 2 9 11, Hachimanyama, Setagaya-ku, Tokyo 156 0056 and* [2)]*Shibaura Meat Sanitary Inspection Station, Bureau of Social Welfare and Public Health, Tokyo Metropolitan Government, 2 7 19 Kounan, Minato-ku, Tokyo 108 0075, Japan*

(Received 29 August 2007/Accepted 21 November 2007)

ABSTRACT. The tonsils of cattle, including palatine tonsils, pharyngeal tonsils, tubal tonsils and lingual tonsils, are designated as specified risk materials (SRM). However, the detailed distribution of lingual tonsils in cattle is unknown. We therefore histologically examined their distribution in 198 tongue specimens from cattle. The examinations confirmed that the presence of lingual tonsils was limited to the tissue of the lamina propria on the dorsal and lateral aspects of the tongue, not reaching the muscular layer below. More than 90% of the lingual tonsils were located between the distribution center of the vallate papillae and the radix linguae (root of the tongue). However, they were also found in the area extending from the lingual torus to the rostral-most vallate papilla in an individual, suggesting that the complete removal of the lingual tonsils requires elimination of the lamina propria extending from the lingual torus to the radix linguae.

KEY WORDS: BSE, cattle, lingual tonsils, specified risk materials (SRM), tongue.

J. Vet. Med. Sci. 70(3): 251 254, 2008

Bovine spongiform encephalopathy (BSE), a type of transmissible spongiform encephalopathy (TSE), was reported first in the U.K. in 1987 [10]. By the end of 2006, more than 180,000 cases had been reported in United Kingdom. Then, the first case of a variant Creutzfeldt-Jakob diease (vCJD) caused by BSE was reported in 1996 [1, 12]. In response to the identification in 2001 of BSE in native-born cattle, active surveillance on all slaughtered cattle started in October of that year in Japan. Up to June 30, 2007, 33 BSE-confirmed cases including the first BSE case were found in Japan.

Eliminating SRM from cattle carcasses is an important measure for protecting human and livestock health from the risk of BSE. In the European Union, the tonsils have been designated as SRM and removed from beef carcasses since 2000 [2]. Also in Japan, the head region with the tonsils have been eliminated in accordance with the Law on Special Measures Against BSE since 2002 [6].

In 2002, the British Food Standards Agency (FSA), using an assay several hundred times more sensitive than the standard assay, found a low level of BSE infectivity in cattle tonsils [7]. As a result, in November of that year, the Ministry of Health, Labour and Welfare of Japan issued a warning not to touch the tonsils while removing the tongue from the head region. Although additional notice to eliminate the lingual tonsils adequately was issued in 2005, this did not involve the descriptions of the concrete existence position in the lingual tonsils.

There are four types of tonsils—palatine tonsils, pharyngeal tonsils, lingual tonsils and tubal tonsils [4]. The palatine and pharyngeal tonsils are visible to the unaided eye. The pharyngeal and tubal tonsils are distributed in the tissue of the rhinopharynx and are therefore removed as a part of the head region. However, the lingual tonsils, which exist in the tongue as histologically independent lymph nodules, cannot be identified macroscopically [8]. Slaughter practices in the U.S. follow the guideline that there are no lingual tonsils rostral to the vallate papilla closest to the radix linguae. Accordingly, during slaughter the tongue is severed at the most caudal vallate papilla and the rostral part is deemed safe for consumption [9]. However, it has been reported that lingual tonsilar material has been found rostral to the most caudal vallate papilla [5]. So far, a detailed description of lingual tonsillar distribution has only been given by Wells *et al.*

Here, we report on our histological examination of the distribution of lingual tonsils in cattle and discuss their removal methods.

MATERIALS AND METHODS

The specimens examined were tongues from 198 cattle removed after slaughter inspection that included a BSE test. The breakdown of samples by age, breed and sex is shown in Table 1. The specimens were divided by age into the following four categories: (1) $x < 12$ months old, (2) 12 months $\leq x < 20$ months, (3) 20 months $\leq x < 30$ months and (4) 30 months $\leq x$. In addition, 15 tongues that had already had the surface mucosa removed for marketing (so-called "peeled tongues") were checked for the persistence of lingual tonsils.

Tongues were refrigerated for 18 hr after slaughter. The tissue examined consisted of the area extending from the tip of the lingual torus to the radix linguae on the left or right lateral aspect, as divided by the dorsal midline. Tongues were cut into 5-mm-wide strips from the center of the most

* CORRESPONDENCE TO: SAWADA, Y., Shibaura Meat Sanitary Inspection Station, Bureau of Social Welfare and Public Health, Tokyo Metropolitan Government, 2 7 19, Kounan, Minato-ku, Tokyo 108 0075, Japan.
e-mail: Yasushi_Sawada@member.metro.tokyo.jp

Table 1. Breakdown of specimens examined

Age in months	Japanese beef cattle			Crossbred cattle			Dairy cattle			Total
	Bull	Steer	Cow	Bull	Steer	Cow	Bull	Steer	Cow	
< 12		1	1			1	6	17		26
< 20					1			28		29
< 30		9	13		11	12		34	3	82
≥ 30		11	15					1	34	61

Breed	Total	Japanese beef cattle	50	Crossbred cattle	25	Dairy cattle	123	198
Sex	Total	Bull	6	Steer	113	Cow	79	

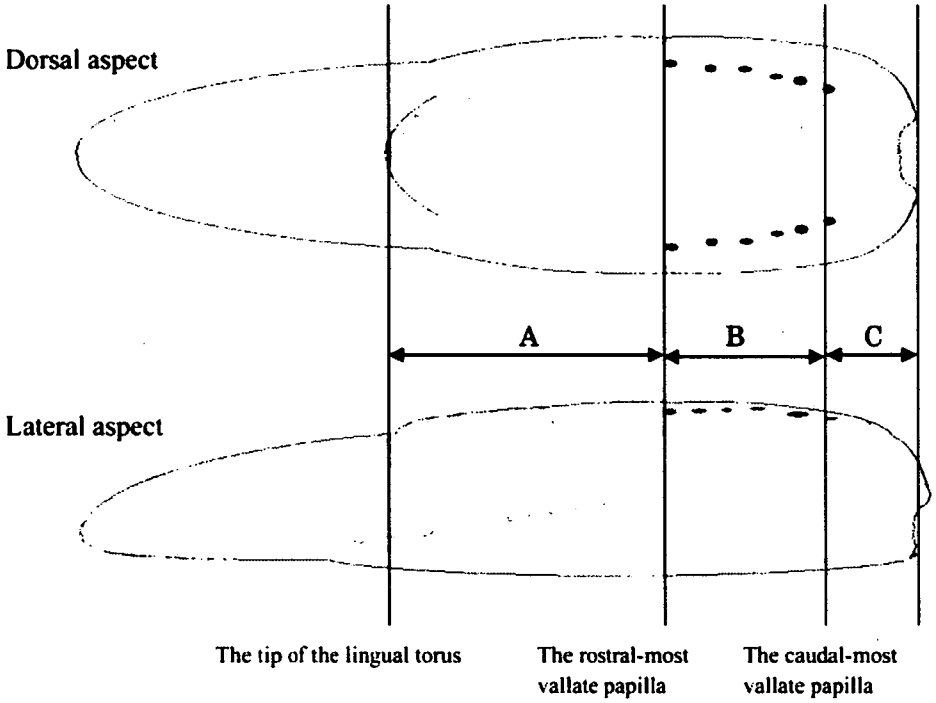

Fig. 1. Areas examined for the distribution of lingual tonsils.

caudal vallate papilla toward the apex linguae (rostrally) or toward the radix linguae (caudally), followed by fixation in 20% formalin. Then, paraffin sections prepared according to a standard method were stained with hematoxylin-eosin (HE) before microscopic observation of the lamina propria and the muscular layer. To account for individual differences in the specimens, the examination area was divided into three parts: area A (closest to the apex linguae) was defined as the area from the tip of the lingual torus to the most rostral vallate papilla (20 specimens), area B was defined as the area from the most rostral vallate papilla to the most caudal vallate papilla (135 specimens), and area C was defined as the area from the most caudal vallate papilla to the radix linguae (63 specimens) (Fig. 1). The body of the tongue was divided into dorsal and lateral aspects.

The presence of lingual tonsils was recognized according to histological criteria, specifically, by finding tissues containing crypts and secondary follicles compartmentalized from their surroundings (Fig. 2), and tissues without crypts but with secondary follicles compartmentalized from the surroundings (Fig. 3) [8].

RESULTS

Detection of lingual tonsils in each area is summarized in Table 2. In all specimens, the distribution of lingual tonsils was limited to the lamina propria and did not extend into the muscular layer. Specimens that had the muscular layer exposed after the removal of the surface mucosa for marketing showed no evidence of lingual tonsillar tissue.

Fig. 2. Lingual tonsils with crypts and secondary follicles.

Fig. 3. Lingual tonsils without crypts but with secondary follicles.

The 20 specimens from area A showed no lingual tonsils on the dorsal aspect, but one specimen (5.0%) contained lingual tonsillar tissue on the lateral aspect. The lingual tonsillar tissue was located midway between the tip of the lingual torus and the most rostral vallate papilla.

In area B, more than 90% of the lingual tonsils were located between the radix linguae and the distribution center of the vallate papillae. However, one specimen contained lingual tonsils at the level of the most rostral vallate papilla. In addition, the presence of lingual tonsils was inversely related to the age of specimen. Of the 135 specimens from area B, 39 (28.9%) contained lingual tonsils on the dorsal aspect and 78 (57.8%) contained them on the lateral aspect.

In area C, most of the lingual tonsils were distributed between the most caudal vallate papilla and the radix linguae; specimens from individuals aged less than 30 months always contained tonsils on either the dorsal or lateral aspect, as well as inconsistently in other locations. Of the 63 specimens from area C, 48 (76.2%) contained lingual tonsils on the dorsal aspect and 60 (95.2%) contained them on the lateral aspect.

DISCUSSION

There are no published reports on the accumulation of prion proteins (PrP) in the lingual tonsils of BSE-infected cattle. However, the tonsils of sheep have shown infectivity or prion accumulation in the case of natural scrapie [3]. For this reason, EC Regulation 999/2001 specifies that the tongue be cut at the lingual torus of the basihyoid bone to avoid food contamination by lingual tonsils. Wells *et al.* [11] reported that intracerebral inoculation of palatine tonsils of cattle experimentally infected orally with BSE ten months earlier caused BSE infection in other cattle. They also pointed out the possibility that tonsils in general are infective. Furthermore, they examined the distribution of lingual tonsils in 100 British cattle tongues marketed for consumption and reported that lingual tonsils were still histologically observed in the tongues after removal of the radix linguae. Similarly, Kühne *et al.* [5] histologically examined the tongues of two cattle aged more than 18 months and reported that lingual tonsils were observed in areas distant from the most caudal vallate papilla.

Our study found that 93.5% of the lingual tonsils were distributed between the most caudal vallate papilla and the

Table 2. Detection of lingual tonsils in each area

Area		Age in months								Total	
		< 12		< 20		< 30		≥ 30			
A[a)]	n	5		5		5		5		20	
	Dorsal aspect	0		0		0		0		0	
	Lateral aspect	0		0		1	(20.0)	0		1	(5.0)
B[b)]	n	26		25		52		32		135	
	Dorsal aspect	7	(26.9)	5	(20.0)	23	(44.2)	4	(12.5)	39	(28.9)
	Lateral aspect	23	(88.5)	18	(72.0)	28	(53.8)	9	(28.1)	78	(57.8)
C[c)]	n	0		4		30		29		63	
	Dorsal aspect	–		2	(50.0)	25	(83.3)	21	(72.4)	48	(76.2)
	Lateral aspect	–		4	(100.0)	29	(96.7)	27	(93.1)	60	(95.2)

a) from the tip of the lingual torus to the most rostral vallate papilla.
b) from the most rostral vallate papilla to the most caudal vallate papilla.
c) from the most caudal vallate papilla to the radix linguae.
The numbers in parentheses indicate detection percentages.

intermediate position between this vallate papilla and the most rostral vallate papilla. However, in rare cases, lingual tonsils were located near the most rostral vallate papilla or even toward the tip of the lingual torus. Thus, our results reconfirmed past reports.

Moreover examination of lingual tonsils located on the dorsal and lateral aspects of the tongue showed that the tonsils were more commonly found on the lateral aspects of the tongue than on the dorsal aspect, but that their distribution was limited to the lamina propria and did not extend into the muscular layer. This finding was confirmed by the fact that no lingual tonsils were found in the specimens with pre-exposed muscular layers. Based on our findings that specimens from individuals more than 30 months old had a low prevalence of detection of lingual tonsils, we suggest that lingual tonsils may regress as animals' age.

Based on the above results, we conclude that the removal of the lingual tonsils designated as SRM would be complete if tongues are processed by completely removing the lamina propria layer extending from the tip of the lingual torus to the radix linguae on the dorsal and lateral aspects. The muscular layer can be safely consumed due to its lack of lingual tonsillar tissue.

The study was carried out with the cooperation of 18 meat inspection centers nationwide. The representatives of the centers are as follows: Kazunori Nakanishi (Asahikawa City Meat Hygiene Inspection Center), Hiroya Oyamada (Towada Meat Inspection Center, Aomori Prefecture), Kesayo Saito (Kenpoku Meat Inspection Office, Tochigi Prefecture), Naomi Onuki (Kensei Meat Inspection Office, Ibaraki Prefecture), Susumu Mabara (Kennan Meat Inspection Office, Ibaraki Prefecture), Masakazu Katayama/Kenji Ono (Toso Meat Inspection Station, Chiba Prefecture), Miyuki Hara (Yokohama City Meat Inspection Center), Aki Shimazaki (Nagoya City Meat Inspection Center), Takayoshi Oba (Toyama Prefectural Meat Inspection Center), Yoshinori Kaji (Kanazawa City Meat Inspection Center), Keiko Fujita (Gifu Prefectural Meat Inspection Office), Shoichi Yamanaka (Matsusaka Meat Inspection Office, Mie Prefecture), Tomoyuki Nakayama (Shiga Prefectural Meat Inspection Office), Hanjiro Kitada (Osaka City Meat Inspection Office), Kazuyuki Okahata (Nishiharima Meat Inspection Office, Hyogo Prefecture), Daisuke Nozaki (Kobayashi Meat Inspection Center, Miyazaki Prefecture), Koichi Yamada / Junko Hamada (Sueyoshi Meat Inspection Center, Kagoshima Prefecture), and Tomoyuki Nanba (Shibaura Meat Sanitary Inspection Station, Tokyo Metropolitan Government).

ACKNOWLEDGEMENTS. We thank Dr. Tetsutaro Sata, director of the Department of Pathology, the National Institute of Infectious Diseases and Professor Hidefumi Furuoka of the Department of Veterinary Pathobiological Science, Obihiro University of Agriculture and Veterinary Medicine for their great advice and comments. This study was conducted as a part of "Studies on food-mediated BSE risk - Development of slaughter methods for preventing the contamination of meat, etc. by the brain and spinal cord tissues" under the Research on Food Safety (17270701), receiving Health and Labour Sciences Research Grants 2005 2006.

REFERENCES

1. Dillner, L. 1996. BSE linked to new variant of CJD in humans. *BMJ.* **30**: 312(7034):795.
2. European Commission. 2000. Commission Decision of 29 June 2000, 418/2000/EC regulating the use of material presenting risks as regards transmissible spongiform encephalopathies and amending Decision 94/474/EC L158/81.
3. Hadlow, W. J., Kennedy, R. C. and Race, R. E. 1982. Natural infection of Suffolk sheep with scrapie virus. *J. Infect. Dis.* **146**: 657 664.
4. Kato, Y. and Yamauchi, S. 2003. Comparative Anatomical Atlas of Domestic Animals. New edition. Yokendo. Tokyo (in Japanese).
5. Kühne, M., Klein, G. and Gasse, H. 2005. Shortening of the bovine tongue according to regulation (EC) 999/2001 is not complying with the current legal definition of specified risk material - a macroscopical and histological preliminary study, *J. Vet. Med. B.* **52**: 102 104.
6. Law on Special Measures Against Bovine Spongiform Encephalopathy (Law No. 70 of June 14, 2002).
7. SEAC Statement. 2003. Statement on BSE risk from bovine tonsil and consumption of Ox tongue.
8. The Viscera of the Domestic Mammals. 1979. Verlag Paul Parey, Berlin, Hamburg. pp. 54 55.
9. USDA FSIS Technical service center: Additional Information & Diagrams Regarding the Removal of Tonsils in Cattle.
10. Wells, G.A., Scott, A.C., Johnson, C.T., Gunning, R.F., Hancock, R.D., Jeffrey, M., Dawson, M. and Bradley, R. 1987. A novel progressive spongiform encephalopathy in cattle. *Vet. Rec.* **121**: 419 420.
11. Wells, G.A., Spiropoulos, J., Hawkins, S.A. and Ryder, S.J. 2005. Pathogenesis of experimental bovine spongiform encephalopathy: preclinical infectivity in tonsil and observations on the distribution of lingual tonsil in slaughtered cattle. *Vet. Rec.* **156**: 401 407.
12. Will, R.G., Ironside, J.W., Zeidler, M., Cousens, S.N., Estibeiro, K., Alperovitch, A., Poser, S., Pocchiari, M., Hofman, A. and Smith, P.G. 1996. A new variant of Creutzfeldt-Jakob disease in the UK. *Lancet* **347**: 921 925.